MSc Program
Environmental Technology & International Affairs



# The Impact of a Potential Future Grand Solar Minimum on Biological Health Effects: Erythema, DNA Damage and Vitamin D Production

A Master's Thesis submitted for the degree of
"Master of Science"

supervised by
Dr. Pavle Arsenovic, MSc

Clara Anastasia Wend, BA, BA

11705235

Vienna, 12.06.2024

# Affidavit

I, **CLARA ANASTASIA WEND, BA, BA**, hereby declare

1. that I am the sole author of the present Master's Thesis, "THE IMPACT OF A POTENTIAL FUTURE GRAND SOLAR MINIMUM ON BIOLOGICAL HEALTH EFFECTS: ERYTHEMA, DNA DAMAGE AND VITAMIN D PRODUCTION", 71 pages, bound, and that I have not used any source or tool other than those referenced or any other illicit aid or tool, and
2. that I have not prior to this date submitted the topic of this Master's Thesis or parts of it in any form for assessment as an examination paper, either in Austria or abroad.

Vienna, 12.06.2024

_____
Signature

# Abstract

Ultraviolet radiation (UVR) emitted by the Sun causes both beneficial and harmful biological responses in humans that are essential for skin and musculoskeletal health. Solar UVR also regulates stratospheric ozone production, which in turn limits UVR transfer to the Earth's surface. This thesis aims to improve the understanding of the relationship between solar activity and biological responses by investigating the impact of a potential 21$^{st}$ century grand solar minimum on three biological health effects: erythema, DNA damage, and vitamin D production. Using the libRadtran radiative transfer model, solar radiation levels at Earth's surface are computed for five distinct levels of solar activity to predict erythemal, DNA damage, and vitamin D radiation doses between 2100 and 2199. This process requires weighting the relevant wavelength bands with their respective action spectra. In relation to the reference scenario of continued prevalent solar activity, a decline of 3.5 or 6.5 $Wm^{-2}$ is found to result in respective relative index increases of 0.72% or 1.18% for erythema, 2.73% or 4.85% for DNA damage, and 1.03% or 1.73% for vitamin D production. Regional differences are also shown to be significant. The greatest relative changes are expected in the midlatitudes: up to 2.12% for erythema, 6.90% for DNA damage, and 3.44% for vitamin D production. Additionally, the northern hemisphere is found to be more affected than the southern hemisphere, displaying 0.45% higher intensity for erythema, 0.98% for DNA damage, and 0.44% for vitamin D production. These findings corroborate expectations derived from future ozone-column simulations. The results also carry important implications for future health protection efforts should a grand solar minimum occur. Education-based measures could prove effective if adapted adequately. However, individual factors play a major role in UV-induced health effects, and thus predictions about overall future impacts on public health remain challenging. Nonetheless, the evidence underscores that efforts to implement effective health protection measures need to be enhanced in a potential GSMi-future given the straightforward and practical prevention strategies available. This is especially true for the northern midlatitudes, where the general population is most at risk and greatest changes would occur.

# Table of Contents

# List of Abbreviations

| | |
|---|---|
| BDC | Brewer Dobson Circulation |
| CME | Coronal Mass Ejection |
| DNA | Deoxyribonucleic Acid |
| EPP | Energetic Particle Precipitation |
| ESA | European Space Agency |
| GCR | Galactic Cosmic Ray |
| GSMi | Grand Solar Minimum |
| KNMI | Royal Netherlands Meteorological Institute |
| MM | Maunder Minimum |
| NH | Northern Hemisphere |
| $NO_x$ | Nitric Oxides |
| ODS | Ozone Depleting Substance |
| RCP | Representative Concentration Pathway |
| SC | Solar Cycle |
| SEP | Solar Energetic Particle |
| SH | Southern Hemisphere |
| TEMIS | Tropospheric Emission Monitoring Internet Service |
| TOC | Total Ozone Column |
| TSI | Total Solar Irradiance |
| UVR | Ultraviolet Radiation |

# Acknowledgements

I am profoundly grateful to my supervisor, Dr. Pavle Arsenovic, for your invaluable guidance and insightful feedback. Additionally, I would like to recognise your generosity in making the necessary data and methodology available to me. Without your expertise and mentorship this thesis would not have been possible.

I would also like to express my deepest gratitude to my parents for their unwavering support, encouragement, and love throughout this journey. Your belief in me has been a constant source of strength and motivation.

A big thank you also goes to my colleagues and friends for standing with me and always lending an ear during these demanding to years.

Thank you all for your contributions to this work and for always being there for me.

# 1. Introduction

*In the centre of all rests the sun… As a matter of fact, not unhappily do some call it the lantern; others, the mind and still others, the pilot of the world.*

-Nicolaus Copernicus, On the Revolutions of the Heavenly Spheres, 1543

The Sun has always fascinated humanity, long before scientists discovered its integral role in "piloting" essential processes on our planet. Solar motifs feature in numerous ancient and modern religions, mythologies and cultures. In Japan, the sun goddess was regarded as the world's supreme ruler and the sun continues to symbolise the Japanese state today. In ancient Egypt, the sun god Re held the primary position among the high gods and sun worship was practiced among Indo-European peoples, Native Americans, Incas, Mayas, and Aztecs, as well as in medieval Iran and ancient Rome (Britannica, T. Editors of Encyclopaedia 2023). These rituals still influence our cultures today. Especially winter and summer solstices are celebrated all over the world. Even religious holidays such as Christmas or St. John's Eve were scheduled to substitute previous traditions of solstice-celebrations given their immense popularity (Ostberg 2023; Eldridge 2023).

Today, we understand the mechanisms that fuelled this fascination. The Sun is a star composed primarily of hydrogen and helium and forms the core of our solar system. Its energy drives the solar system, and the interactions between the Sun and Earth, determined by Earth's unique position make life on our planet possible and determine its atmosphere, temperature, and geography. This distance at 150 million kilometres from the Sun allows for the existence of liquid water, photosynthesis, and, consequently, life (Hossain 2023). The Sun not only creates, but also shields life from its harmful ultraviolet radiation (UVR) by facilitating the photochemical reactions leading to stratospheric ozone formation. This so-called ozone layer absorbs the majority of harmful UV radiation and thus limits its incidence on the Earth's surface (Dessler 2000).

Solar radiation thus determines the formation of stratospheric ozone. However, the Sun is a variable star undergoing a regular 11-year cycle that alternates between minimum and maximum activity, as well as extended periods of disproportionally high or low activity. These periods are called grand solar maxima and minima (Hathaway 2015). Numerous

studies predict solar activity to experience a grand solar minimum in the near future (Abreu, Beer, and Ferriz-Mas 2010; Lockwood et al. 2011; Roth and Joos 2013; Steinhilber and Beer 2013). Such a reduction in solar UVR would result in lower oxygen photolysis and, thus, lower levels of stratospheric ozone formation (Gray et al. 2010). In fact, studies (Arsenovic et al. 2018) have suggested a paradox conclusion: lower solar irradiance leads to higher incidences of UV on the Earth's surface.

UVR is harmful because it is the primary cause of a high incidence of disease in the world, namely skin cancer, with more than 1.5 million new cases diagnosed in 2022 (International Agency for Research on Cancer and WHO, n.d.). A large body of literature has conducted extensive research on the interactions between ultraviolet radiation and human health, especially skin-related conditions. The most relevant skin-related dangers to human health are erythema (sunburn) and damage to deoxyribonucleic acid (DNA). But solar UVR also has benefits, namely through facilitating the production of vitamin D, which is necessary for several important bodily functions (Lucas et al. 2006). The majority of research on UVR and health assumes the prevalence of constant solar activity. But given the interactions between solar activity and ozone formation, a potential future grand solar minimum can be expected to have significant impact on UV-related health effects in humans. To date, the potential health implications of a possible future minimum have not been assessed. This thesis aims to bridge this gap by exploring how a grand solar minimum would impact erythema, DNA damage and vitamin D production in humans.

Investigating these effects is of relevance because of their profound implications for public health. As mentioned, erythema and DNA damage are critical precursors of skin cancer, which increasingly strains health systems worldwide. On the other hand, vitamin D has numerous positive effects on human health, especially on the musculoskeletal system (Lucas et al. 2019). Promoting responsible behaviour regarding UV-exposure that ensures a balance between its positive and negative aspects is important under all solar conditions. However, this thesis looks at how this balance might potentially be altered in the future. It can thus act as an important preliminary assessment to allow for better public health planning and risk mitigation in the future, subsequently ensuring that potential health hazards are addressed proactively in the face of changing solar conditions.

Following this brief introduction, an extensive literature review examines the state of the art regarding research on solar activity measurement, sun-climate-atmosphere interactions, and the biological mechanisms underlying UV-related health effects. This review sets the stage for presenting the research question and objectives in chapter 3. Chapter 4 outlines the methodology used in the study, detailing the models and analytical techniques employed to measure future radiation doses. Chapter 5 entails a thorough description of the results, which is followed by an elaborate discussion in the final chapter, outlining the implications of the findings, how they relate to previous research, and possible applications in the future.

# 2. State of the Art

## 2.1. Solar activity: The solar cycle and its extremes

In comparison to other stars, the Sun's luminosity, which is a measure of the amount of light an object emits per unit of time (Gregersen 2015), is relatively constant. Nonetheless, solar activity alternates over an 11-year cycle called Schwabe cycle. This cycle results from a reversal of the Sun's magnetic field occurring every 11 years. Solar magnetic activity is spawned by an oscillatory hydromagnetic dynamo below the Sun's surface (Abreu, Beer, and Ferriz-Mas 2010). It has been observed that solar activity is proportional to the dark areas on the Sun called sunspots. However, it is more accurately conceived as total solar magnetic activity, including the open and closed solar magnetic field (Usoskin 2023). Solar activity thus encompasses solar radiation, as well as solar phenomena. Solar radiation is measured in total solar irradiance (TSI) which alternates over the Schwabe cycle at an amplitude of approximately 0.1% (NASA Science Editorial Team 2013)

Solar phenomena include sunspots, solar flares, and solar winds. Sunspots are regions on the Sun's surface that appear darker because they are cooler than their surroundings, which arises from their strong magnetic fields that well up to their photosphere. This can also result in solar flares, which are violent explosions that occur due to increasing complexity of the Sun's magnetic fields (Rapp 2010; Hossain 2023). Solar wind, consisting of plasma, is also continuously emitted by the Sun and carries solar magnetic fields, also called the heliosphere (Gray et al. 2010; Steinhilber and Beer 2013). Massive explosions of solar wind (plasma) are called coronal mass ejections (CME), as they are ejected from the corona, the Sun's outer layer. If solar plasma interacts with atmospheric oxygen and nitrogen molecules, energy is released in the form of photons, observable as auroras. Usually, the Earth's magnetic field prevents solar winds entering the atmosphere. However, magnetic field lines diverge at the poles, allowing penetration of solar plasma (Hossain 2023). In terms of the solar cycle, solar minima correspond to periods of low solar activity, i.e. low TSI, weak solar winds, and low number of sunspots, solar flares, CMEs and auroras. The opposite is true for solar maxima (Rapp 2010; Thomas 2020; National research council 2012; NASA Science Editorial Team 2017). The structure of the Sun and its phenomena are depicted in Figure 1.

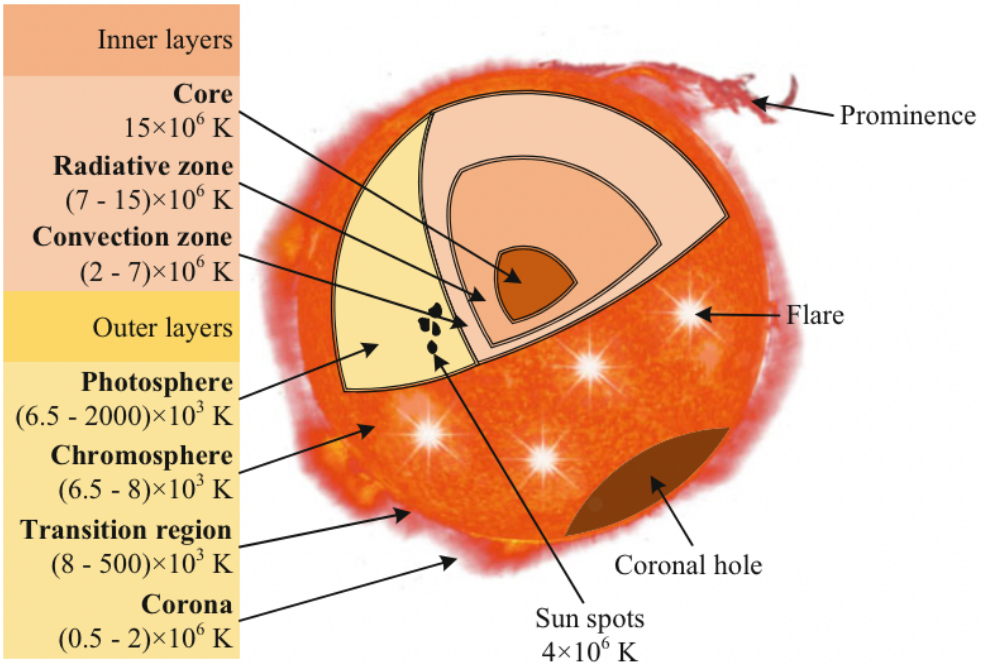


**Figure 1**: Cross Section of the Sun (Hossain 2023, 9)

Besides the regular 11-year cycle, there also periods of extended higher or lower solar activity, referred to as grand solar maxima and minima. The largest Grand Solar Minimum (GSMi) from recent Earth's history occurred between AD 1650 and 1715 and was called the Maunder Minimum (MM). During such a GSMi, solar magnetism, sunspot numbers, and TSI all decrease – the entire solar cycle weakens. During the MM, sunspots almost completely disappeared (Lockwood et al. 2011; Usoskin, Solanki, and Kovaltsov 2011; Usoskin 2023; Abreu et al. 2008). This reduced solar activity results in lower TSI, and thus a deficit in the Earth's energy budget. In fact, the Maunder Minimum coincided with the "Little Ice Age", a period of cooling in the Northern Hemisphere where mean annual temperatures decreased by 0.6 K (Jackson and Rafferty 2024). Although part of this cooling may have been caused by the higher volcanic activity resulting in aerosol cooling, and ocean circulation shifts, lower solar activity had a significant contribution (Jackson and Rafferty 2024; NASA Science Editorial Team 2020; 2019). Figure 2 shows the historical time series of TSI. The periodicity of the 11-year solar cycle is evident, as well as the extended periods of lower solar activity during the MM and the subsequent GSMi, the Dalton Minimum (1790–1830).

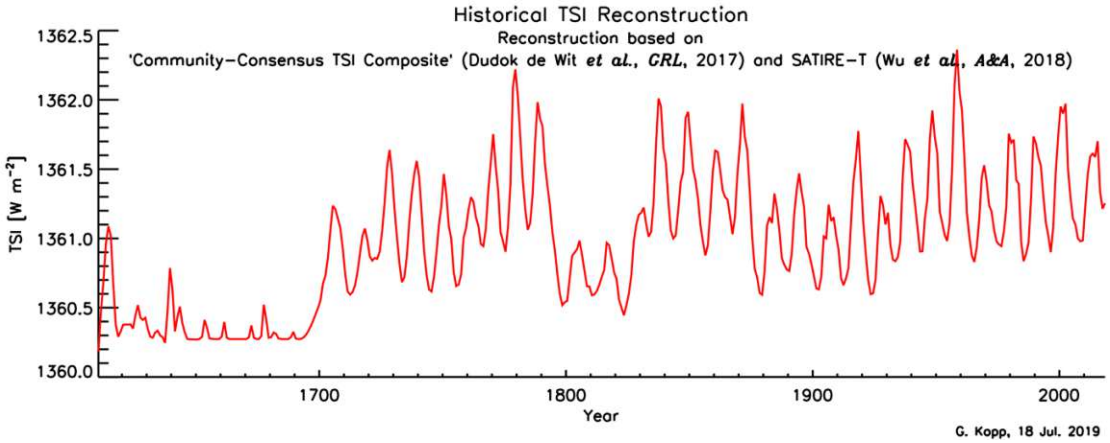


**Figure 2**: Historical TSI Reconstruction (Kopp and University of Colorado 2019)

## 2.2. Measuring solar activity

Since 1978, exact measurements of TSI have been conducted using modern satellite technology. However, the systematic observations of solar activity begun with the invention of the telescope in 1610. They are primarily records of sunspot numbers and solar cycle lengths (Gray et al. 2010). The International Sunspot Number, $R_I$, is the most relevant indicator of solar activity due to its long availability (Hathaway 2015). It was first developed by Johann Rudolf Wolf as a relative sunspot number ($R_Z$) because he did not employ individual sunspots but rather sunspot groups (it is also called Wolf or Zürich Sunspot Number). It is based on observations between 1849 and 1981. The approach was significantly improved by Hoyt and Schatten (1998), who devised an index counting number of sunspot groups, averaging records of multiple observers and normalising those results to the International Sunspot Numbers. This approach allows extrapolation to 1610 using pre-Wolf records and proxy data (Hathaway 2015; Usoskin 2023; Gray et al. 2010). Nonetheless, new findings may make corrections of solar activity reconstruction necessary (Arlt 2008; Vaquero 2007).

To make accurate predictions of future solar activity, data reaching back into the 17$^{th}$ century is not sufficient. Cosmogenic isotopes can be used as a proxy to infer information on longer timescales. Galactic cosmic rays (GCR) are high energy particles materialising from outside the solar system. The GCR are modulated by the heliosphere (the Sun and its magnetic field), which shields the Earth from those particles. Therefore, the GCR precipitation peaks when the solar activity is low (Bazilevskaya et al. 2008). Upon penetrating Earth's atmosphere, some GCR-particles collide with atmospheric gases,

forming radioactive isotopes, also called cosmogenic radionuclides (Usoskin, Solanki, and Kovaltsov 2011). As some of these cosmogenic isotopes do not have terrestrial sources, they allow conclusions about solar activity. Therefore, solar activity can be reconstructed by analysing isotopes stored in natural archives (Usoskin, Solanki, and Korte 2006; Abreu et al. 2008; Gray et al. 2010; Usoskin 2023).

Cosmogenic radionuclides $^{14}C$ and $^{10}Be$ are the most important indicators for solar activity reconstruction. Radiocarbon $^{14}C$ is produced through collision with $^{14}N$ nuclei in the upper troposphere, after which it is oxidised to $CO_2$ and enters the carbon cycle. Measurements are taken from annual tree rings of tree-trunk samples (Roth and Joos 2013). The carbon cycle's global nature dismisses regional climatic effects (Hathaway 2015). Isotope $^{10}Be$ is produced through collision with atmospheric N, O and Ar in the lower stratosphere, where it attaches to aerosols and then precipitates to surface Earth (Kovaltsov and Usoskin 2010). The concentrations of $^{10}Be$ can then be measured in polar ice cores. Precipitation mostly occurs in midlatitudes, making $^{10}Be$ reflect regional effects (Steinhilber and Beer 2013; Usoskin, Solanki, and Kovaltsov 2011; Lockwood et al. 2011; Shapiro et al. 2011). These records can be used to reconstruct TSI for over 9,000 years using solar modulation potential $\Phi$, which describes the strength of GCR flux (Lockwood 2010; Lockwood et al. 2011; Barnard et al. 2011; Abreu, Beer, and Ferriz-Mas 2010; Väisänen et al. 2023). By averaging numerous radionuclide records rather than using individual data sets, reconstruction can be made more robust and it has been shown that 70% of variability in the cosmogenic record results from solar activity, while 30% reflects climate effects (Steinhilber et al. 2012).

Combining direct measurements of sunspots and proxy data from radionuclides allows inferences about past and future solar activity. Sunspot numbers also serve as a calibration tool for the long-term proxies (Clette et al. 2007). Statistical analyses can be conducted on the reconstructed data to detect regular features about solar activity and GSMi in particular, as the extended time series displays numerous minima in addition to the Maunder Minimum covered in sunspot data. The fact that the cosmogenic reconstruction between 1600 and today coincides with the sunspot data reflects the robustness of this method (Abreu, Beer, and Ferriz-Mas 2010). GSMi display a variety of patterns. Usoskin, Solanki and Kovaltsov (2007) define GSMi as periods with a sunspot number below or equal to 15 for at least 20 years or forming a clear decline where the lowest point is below

or equal to 20 sunspots. Using this definition, they identified 27 grand minima during the Holocene (since 9500 B.C.E). This corresponds to ca. 17% of total activity which the Sun spends in minimum state. Abreu, Beer and Ferriz-Mas (2010) use a slightly different definition; they posit that the Sun spends 20% in minimum activity due to the normal distribution of solar modulation potential Φ. Furthermore, minima have been found to cluster every 2000-3000 years. Within these clusters, minima occur quasi-periodically around every 200 years. However, their occurrence is determined by stochastic or chaotic processes. Finally, Maunder-type minima last for approximately 100 years (Usoskin, Solanki, and Kovaltsov 2011; Abreu, Beer, and Ferriz-Mas 2010). Figure 3 displays the reconstructed sunspot numbers for the past 9400 years showing the trends discussed above.

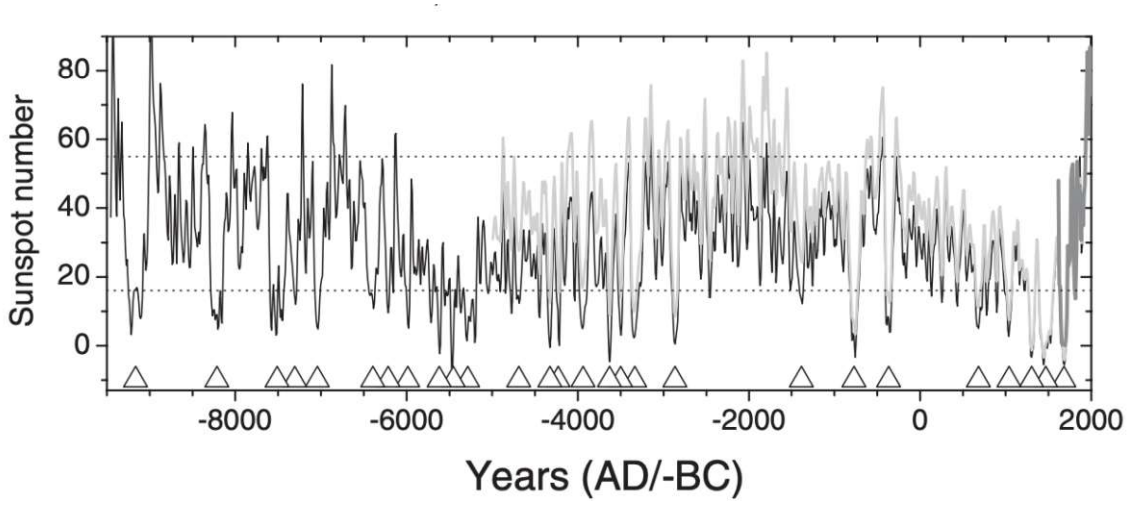


**Figure 3**: Reconstructed sunspot numbers 9400 BCE-2000 AD (Usoskin, Solanki, and Kovaltsov 2011, 373)

Predicting future solar cycle behaviour is difficult because the Sun's non-linear dynamo is hard to model (Schuessler 2007). Cycle statistics or geomagnetic precursors offer an alternative (Hathaway 2015). Abreu et al. (2008) for instance used statistical distribution analysis to predict the duration of the modern grand maximum we had been experiencing since 1940. In 2008, they concluded that it would last another 15-36 years, and in fact, observations show decreasing activity in the cycles since then. They also predicted a 40% probability the modern grand maximum would be superseded by a GSMi. Abreu, Beer and Ferriz-Mas (2010) revised these conclusions, predicting an end of the modern grand maximum in 2020 and the onset of a grand minimum within 100 years. Such statistical properties could be incorporated into solar dynamo models to improve their reliability.

Lockwood (2010), too, assessed past variations of solar modulation potential $\Phi$ and made an analogue forecast of its future evolution. He found that the chance of solar activity falling below MM-conditions within 40 years is 8%. This chance however rises to 43% within the next 100 years. Barnard et al. (2011) expanded this prediction to include sunspot numbers besides solar modulation potential. Lockwood et al. (2011) show that group sunspot numbers and solar modulation potential have a reliant level of predictability for solar activity. They also remark that current declines in peak and mean group sunspot numbers are greater than in any time after the MM. Prediction of a new GSMi also remain robust when using averaged radionuclide records as in Steinhilber and Beer (2013). They predict solar activity for the next 500 years employing two methods that differ in their handling of observed amplitude modulation: The first method overlooks it completely and makes predictions based on the most significant historical periodicities assuming continuous phases, while the second method uses a wavelet decomposition and an autoregressive model to account for amplitude modulation. Both methods predict a minimum around 2100 A.D. with the prior forecasting a duration of 50 years and subsequent higher activity, and the latter forecasting a duration of 100 years and subsequent moderate activity. Overall, the literature agrees that a modern grand minimum may occur in the near future, reaching minimum TSI values around the year 2100 (Abreu, Beer, and Ferriz-Mas 2010; Steinhilber and Beer 2013).

## 2.3. Solar Influences on Atmosphere and Climate

### 2.3.1 Temperature

Analysing and predicting solar activity is relevant because it drives various climatic processes on Earth. During the MM, TSI was approximately 3-4 W/m$^2$ below today's levels, which corresponds to a solar radiative forcing of approximately 0.5-0.7 W/m$^2$ (Shapiro et al. 2011). Given that solar radiation is the main driver of the Earth's energy budget and both the Maunder and Dalton minima coincided with periods of extended surface cooling, many studies have looked at the relationship of reduced solar radiation on temperature. According to Anet et al. (2014), a large proportion of cooling between 1780 and 1840 can in fact be attributed to low solar activity (next to other natural forcings such as volcanic aerosols). Even though there are some authors that argue a new GSMi in the 21$^{st}$ century will even lead to new "Little-Ice-Age"-conditions (Abdussamatov 2016; Zharkova 2020), the general consensus within the scientific community is that the

anthropogenic greenhouse effect largely outweighs any reduction in radiative forcing (National research council 2012). Anet, Rozanov, et al. (2013) for instance predict a reduction of global mean surface warming by 0.2 to 0.3 K between 2081–2100 assuming a modern GSMi. These results are corroborated by other studies using different climate models and reference scenarios that find reduced warming in the range of 0.25 to 0.5 K (Feulner and Rahmstorf 2010; Rozanov et al. 2011; Meehl, Arblaster, and Marsh 2013). Arsenovic et al. (2018) investigated GSMi-scenarios with different durations. Their results show a 0.3 K difference in global surface temperature for a duration until 2099 and a 0.6 K difference for a duration until 2199, which compensates approximately 25% of projected global warming under Representative Concentration Pathway (RCP) 4.5. Should the minimum recover to regular activity, only 4% of anthropogenic warming would be compensated by 2199. Their results also show regional differences in the temperature response, namely polar amplification. Figure 4 clearly demonstrates that while there has been alignment of TSI intensity and global surface temperature before the industrial revolution, this effect has been largely outweighed by anthropogenic warming since then.

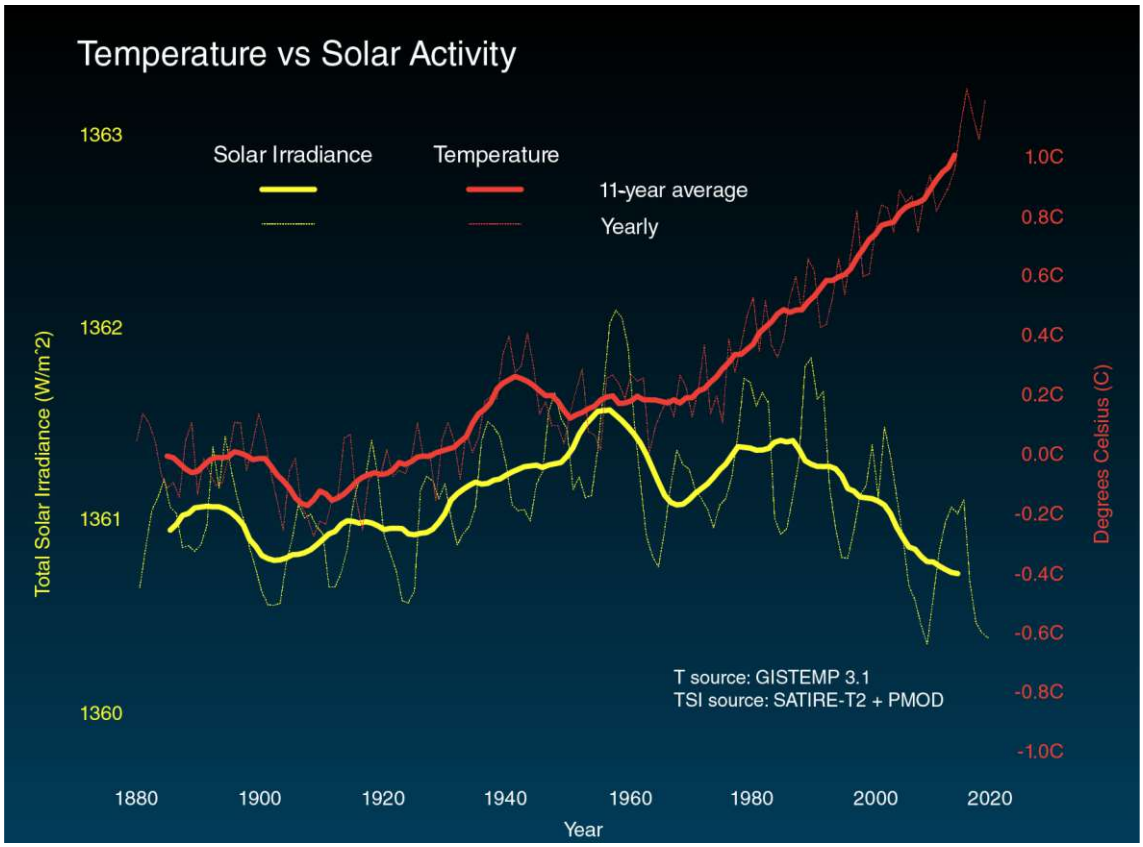


**Figure 4**: Temperature vs. Solar Activity 1880-2020 (NASA Science Editorial Team 2020)

Other relationships between solar activity and climate include variations in winds, clouds, precipitation, sea surface temperatures, the North Atlantic Oscillation (NAO), or the Brewer-Dobson Circulation (BDC) (Gray et al. 2010; Anet et al. 2014; Ineson et al. 2015; Arsenovic et al. 2018; Martin-Puertas et al. 2012). Furthermore, solar activity influences several atmospheric gases that subsequently interact with solar radiation through aerosols or clouds, for example nitric oxides ($NO_x$), OH radicals, methane or water vapour (Madronich and Flocke 1999). As energy from different bands of the solar spectrum is absorbed at different parts of the atmosphere, solar radiation cannot be considered as a single forcing. For instance, TSI directly impacts the surface, while UV and solar energetic particles (SEPs) directly impact the stratosphere und thus require feedback mechanisms to impact the surface (Gray et al. 2010). These forcing mechanisms are depicted in Figure 5. Most importantly for this research, it shows how ozone is influenced by UV and indirectly by SEPs through NOx, as well as through Arctic and North Atlantic Oscillation.

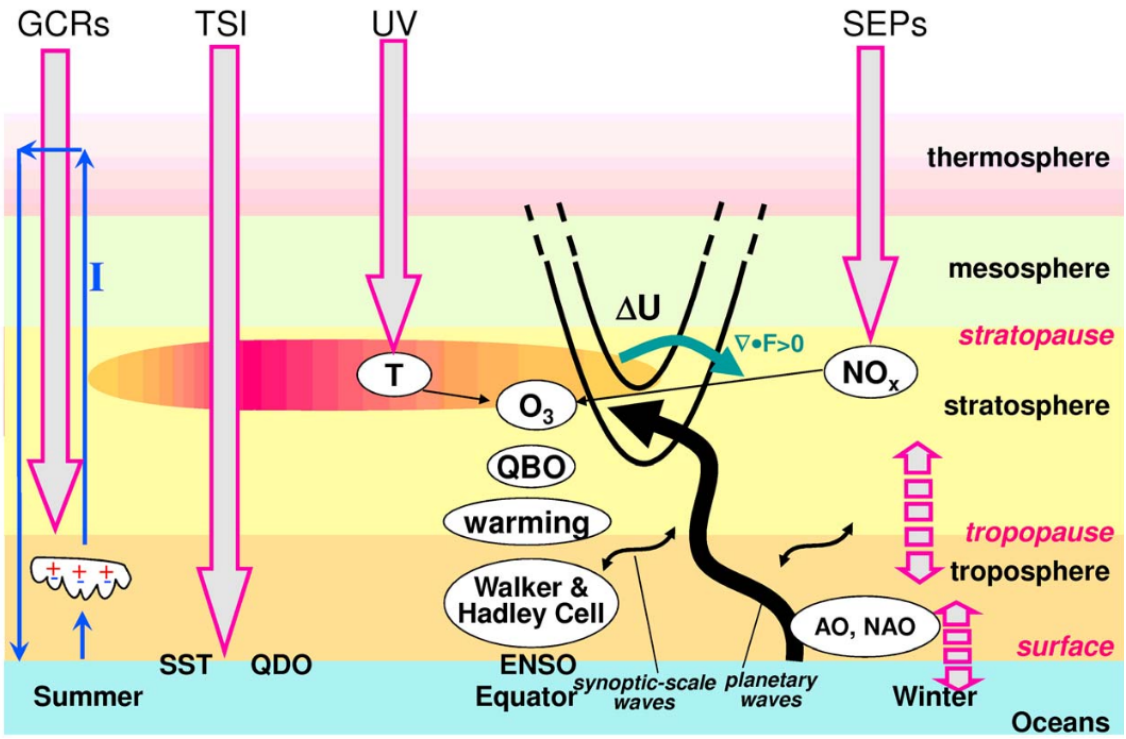


**Figure 5**: Solar Forcing Mechanisms (Gray et al. 2010, 25)

SST: Sea surface temperature, T: Temperature, QDO: quasi-decadal oscillation, QBO: quasi-biennial oscillation, ENSO: El Niño Southern Oscillation, AO: Arctic Oscillation, NAO: North Atlantic Oscillation

### 2.3.2. Ozone

Another important climate effect of solar variability is its impact on ozone production, which can be induced directly and indirectly. As ozone is essential for radiative heating of the stratosphere, its production influences the stratosphere's radiative balance and indirectly impacts circulation (Gray et al. 2010). Three solar-induced mechanisms are central for changes in stratospheric ozone. First, ozone is produced via oxygen photolysis of molecular oxygen; a two-step process in which UV light dissociates molecular oxygen $O_2$ to 2O. Each of these atoms then bonds with molecular oxygen to form ozone $O_3$ (Dessler 2000; Lockwood 2010). Second, energetic particle precipitation (EPP), originating from solar activity, can indirectly impact ozone concentrations through producing odd nitrogen and odd hydrogen species. This subsequently amplifies ozone reduction cycles: e.g. $NO + O_3 \rightarrow NO_2 + O_2$; $NO_2 + O \rightarrow NO + O_2$ (Gray et al. 2010; Anet, Muthers, et al. 2013; Maycock et al. 2015; Arsenovic et al. 2018). Third, these ozone destruction cycles can be decelerated by stratospheric cooling resulting from decreased UV (Anet, Muthers, et al. 2013). Fourth, indirect circulation effects can alter

transport patterns of ozone and lead to regional depletion in the tropics (Gray et al. 2010; Arsenovic et al. 2018)

Considering these chemical processes, reduced solar activity results in lower ozone production levels. In fact, Anet, Muthers, et al. (2013) found that ozone decreased in the ozone layer by 8% during the Dalton Minimum – a result of the interaction of various forcings, namely volcanic, UV solar spectral and EPP. Based on these findings, they propose a reduction in total ozone column (TOC) up to 7% for a GSMi-scenario in the 21st century. Anet, Rozanov, et al. (2013) predict a delay in ozone recovery of 10 years or longer, corresponding to differences of up to −20 Dobson Units (DU) between a GSMi and reference scenario (REF), where REF refers to continued regular solar activity. They also predict a stronger decrease over midlatitudes than polar or equatorial regions. These results are corroborated by Maycock et al. (2015) who assume a 6%-decrease in ozone at the tropical stratopause for 2050-2099. Rozanov et al. (2011) also conclude delays in ozone recovery. They include anthropogenically induced total ozone recovery into their analysis and find that this is offset by solar forcing effects. Regional differences are also significant with the strongest effects outside the polar regions. But even here, 30-40% of ozone recovery is compensated by reduced stratospheric ozone recovery. Arsenovic et al. (2018), too, predict a 8%-decrease in stratospheric ozone in a MM-like scenario. Again, regional differences persist, with midlatitudes showing the greatest decrease of up to −20 DU (4%).

In REF, TOC increases globally. Yet, Brewer-Dobson-Circulation is expected to accelerate, leading to increased transport of ozone-rich air away from the tropics towards the midlatitudes. Several authors have commented on such extra-tropical ozone recovery (Austin and Wilson 2006; Shepherd 2008; Waugh 2009; Li, Stolarski, and Newman 2009). Additionally, the polar vortices prevent mixing of non-polar air with polar air further facilitating the amassment of ozone-rich air in the midlatitudes (Arsenovic et al. 2018). In GSMi-scenarios these effects are counteracted on the one hand by reduced oxygen photolysis. On the other hand, lower ocean surface temperatures caused by reduced solar radiation decelerate the BDC, offsetting 30-50% of TOC-increase in the Northern hemisphere (NH). Additionally, polar vortices become weaker, allowing more ozone to reach the poles (Arsenovic et al. 2018). BDC deceleration affects the Southern hemisphere (SH) to a lesser extent, making it more stable in relation to changes in solar

activity and remaining more sensitive to reductions in ODSs (Zubov et al. 2013). The spatial distribution of total ozone column difference for future minus present conditions can be seen in Figure 6. Diagram (a) depicts to a reference scenario, while diagram (b) depicts a MM-like scenario. The colour intervals represent 10 Dobson Units and are significant to the 95% confidence interval.

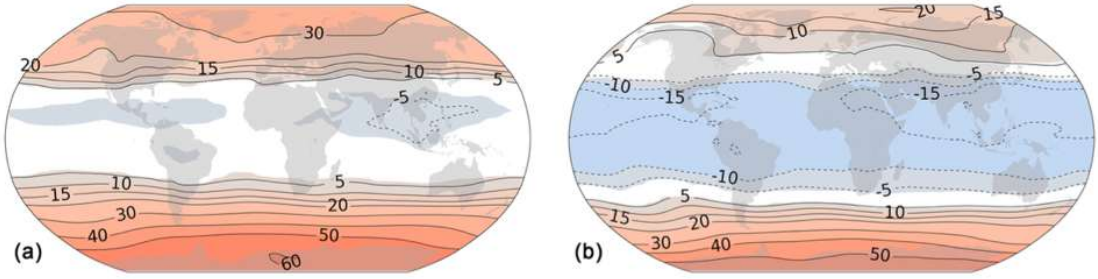


**Figure 6**: Spatial Distribution of Future Ozone Column (Arsenovic et al. 2018, 3478)

Stratospheric ozone is essential in regulating UV radiation on Earth's surface because it is an excellent absorber of UV photons (Aucamp, Björn, and Lucas 2011). The ozone-UV relationship has become a well-publicised societal issue since the seminal discovery of Farman, Gardiner, and Shanklin (1985) who showed the dramatic reduction of ozone levels over Antarctica between the late 1950s and mid-1980s (a 50% reduction in TOC). This depletion was attributed to the accumulation of anthropogenic chlorofluorocarbons in the stratosphere. (Dessler 2000). What became known as the "ozone hole" gained such political traction that it culminated in the adoption of the 1987 Montreal Protocol on Substances that Deplete the Ozone Layer. 198 states agreed to cease production of ozone-depleting substances (ODSs) in this exceptional example of international environmental legislation (Solomon 2019). The Montreal Protocol has been largely successful. In its latest Scientific Assessment of Ozone Depletion, the World Meteorological Organization (WMO, 2022) announced a continued decrease in atmospheric concentrations of ODSs. The report also expects a return to 1980-TOC levels around 2066 in the Antarctic, 2045 in the Arctic, and 2040 for latitudes between 60°N and 60°S. However, these values assume constant solar activity and do not account for the impact of a GSMi, which would likely delay this recovery as discussed above.

## 2.4. UV Radiation and Human Health

The Sun's electromagnetic spectrum covers a large range of wavelengths spanning from radio waves to gamma rays (Babatunde 2012). But 99% of this radiation is emitted in the wavelength bands between 150 to 4000 nm, i.e. in form of UVR, visible light, and infrared radiation (Bhatia 2014). Overall, ultraviolet radiation represents only 6.1% of the solar spectrum (Schuch et al. 2013). It spans the wavelengths between 100 to 400 nm and can itself be separated into UVC (100–280 nm), UVB (280–315 nm), and UVA (315–400 nm) (Aucamp, Björn, and Lucas 2011). UVC radiation is completely retained in the stratosphere, making UVA and UVB radiation the only natural radiation forms relevant to human health (Flo et al. 2017). Additionally, 90% of UVB are absorbed by ozone and oxygen in the atmosphere, while UVA can pass through. Subsequently, UVA represents 95% of UVR reaching Earth and UVB corresponds to 5% (Lucas, Prüss-Üstün, and Perkins van Deventer 2010; Schuch et al. 2013). Besides solar radiation, ambient UVR also depends on atmospheric constituents (ozone, clouds, aerosols), the Earth's albedo, the solar zenith angle (Sun's angle of incidence), and altitude. Ozone, clouds, and aerosols block UV from reaching the surface through their absorptive qualities. The solar zenith angle determines the distance and thus the amount of atmosphere radiation has to travel through to reach the surface. Altitude has the same effect. Finally, albedo influences how much energy is immediately reflected and how much is absorbed (Bais et al. 2019; Laschewski and Matzarakis 2023). Highest ambient UVR can thus be found in regions near the equator, in clear-sky conditions, around middays in the summer months.

Solar energy is often said to be powering life on Earth as it drives the climate, water cycle and photosynthesis. However, solar radiation, more specifically, UVR, has been shown to have multiple effects on human health. In fact, the whole UV spectrum has been classified as carcinogenic to humans (El Ghissassi et al. 2009). Skin cancers, for which UVR is the primary cause, are also responsible for approximately 120,000 deaths per year (WHO 2022). But there are positive impacts too, most notably UV's role in vitamin D production. In a comprehensive review, Lucas et al. (2006) analysed global burdens of disease from UV radiation and found that UV-related health impacts span immune effects, effects on the eyes, and effects on the skin. Overall, they identified 25 independent possible pathways of varying levels of causality evidence. These pathways are summarised in Figure 7. Distal factors describe the environmental factors causing

variance in UVR levels reaching the ground. Proximal factors describe individual characteristics influencing the level of UV absorption in humans which can be behavioural, genetic, cultural or related to the constitution of the immune system. The column on the right then names the numerous diseases that can be caused by extended UV exposure. UV-related health issues are thus caused by a complex interaction of climate, environmental, behavioural and genetic factors.

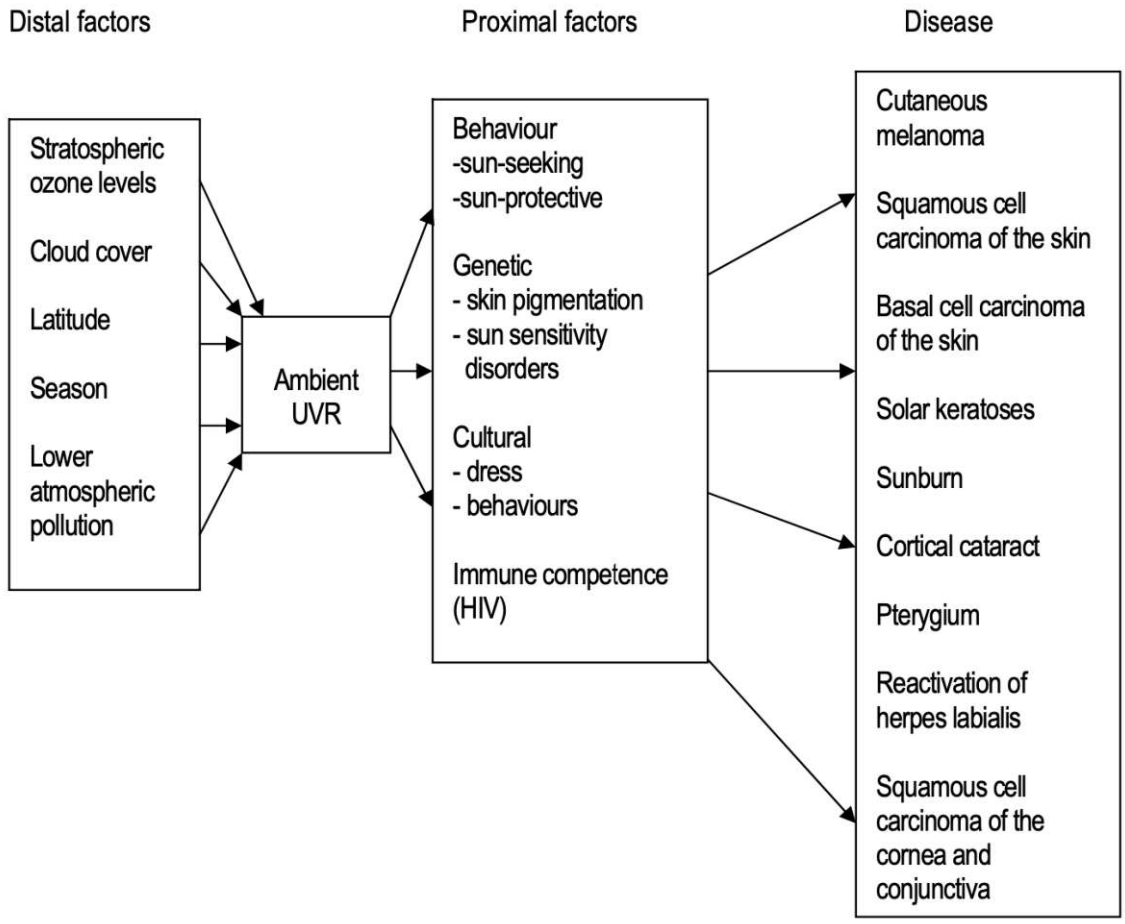


**Figure 7**: Pathways of UV-induced health damage (Lucas et al. 2006, 3)

UV-induced health effects on the skin have been most thoroughly assessed and provide the strongest evidence for causality (Malinović-Milićević et al. 2022). UVA and UVB damage human skin differently (Yang et al. 2023). UVA deeply penetrates several layers of skin: the cuticle, the epidermis, and the lower dermis (Ansary et al. 2021). UVB mainly penetrates the epidermis and superficial dermis. However, the higher energy of UVB's shorter wavelengths increases the level of damage it can inflict on the epidermis (Sklar et al. 2012; Gupta et al. 2013). These mechanisms are displayed in Figure 8. The different impacts of UVA and UVB on the skin are relevant concerning their action spectra, which

measure how effective different wavelengths are in driving a photobiological process (Urbach 2001). The different photobiological processes that will be assessed here are erythema, DNA damage and vitamin D production. The UVB waveband is the most effective for all three and has been shown as the main causative waveband, while the UVA waveband shows reduced effectiveness for erythema and DNA damage but none for vitamin D (Schuch et al. 2013; Lucas et al. 2018).

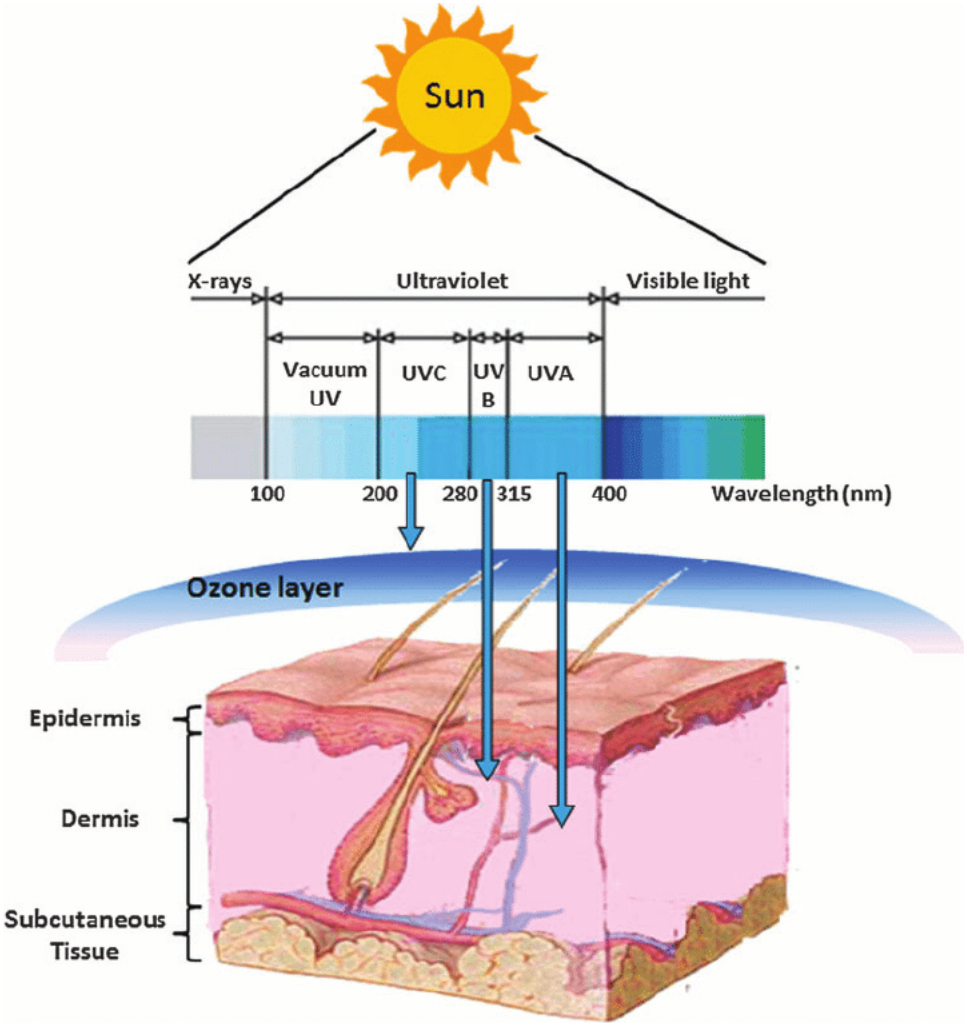


**Figure 8**: Wavelength-Dependent Skin Damage Mechanisms (Gupta et al. 2013, 424)

### 2.4.1. Erythema

Erythema refers to the reddening of the skin following exposure to UVR and is commonly referred to as sunburn. It is caused by increased blood volume which can result in an inflammatory response in the form of swelling (oedema), and an increase in white blood cells (Benrath, Gillardon, and Zimmermann 2001). Erythema can arise in numerous

forms. Under some genetic conditions, they can lead to photo dermatoses, which are inflammatory skin disorders. Additionally, overexposure can result in photoaging (wrinkling) and actinic keratosis (scaly spots). Furthermore, erythema is a significant risk factor for skin cancers (Lucas et al. 2006; 2018; 2019; Yang et al. 2023).

### 2.4.2. DNA Damage

Skin cancers develop due to prolonged UV-induced DNA damage, inadequate DNA repair, and UV-induced immunosuppression (Lucas et al. 2019). Hence, DNA damage is a vital mechanism to understand. DNA is capable of absorbing both UVA and UVB and since UVA can penetrate deeper, it can reach layers that contain dark pigment-producing melanocytes and dividing stem cells. UVA indirectly modifies DNA by catalysing a series of reactions resulting in DNA oxidation. This is a possible mechanism explaining DNA single strand breaks (Schuch et al. 2013). Furthermore, DNA oxidation can trigger damage to other cell structures like lipids and proteins, which can then cause cells to die off or form mutations (Moysan et al. 1993).UVB is directly absorbed by DNA and then interferes with the bonding of its bases, resulting in defective bonds that inhibit transcription, replication, and protein synthesis. Usually, DNA is repaired by a polymerase that detects the lesions and removes the damaged parts. If this does not occur, the result can be cell death, mutations or carcinogenesis (Sinha and Häder 2002; Rastogi et al. 2010).

As mentioned before, DNA damage can cause skin cancer. In fact, skin cancers are the most prevalent types of cancer worldwide (Lucas et al. 2019). In 2022, over 1.5 million new cases were diagnosed (International Agency for Research on Cancer and WHO, n.d.). As UV is the precursor for DNA damage, van Dijk et al. (2013) assessed the extent of skin cancer risk avoided by the Montreal Protocol. They concluded that the difference between a protocol- and no protocol-scenario amounted to two million skin cancer cases per year. There are three types of UV-induced skin cancer: cutaneous malignant melanoma, keratinocyte cancers (squamous cell and basal cell), and Merkel cell carcinoma (Lucas, Prüss-Üstün, and Perkins van Deventer 2010; Lucas et al. 2019). UVR is the primary cause of both cutaneous malignant melanoma, and keratinocyte cancers. Notably, the entirety of keratinocyte cancers in Australia was attributed to UV exposure (Olsen et al. 2015). While cutaneous malignant melanoma caused 57,000 deaths in 2020

(De Pinto et al. 2024), keratinocyte cancers do not have such a high mortality. They can however incur high health system costs due to their prevalence – in the USA for instance, their treatment constituted 5% of total healthcare expenditure between 2007 and 2011 (Guy et al. 2015). Merkel cell carcinomas, although rare, are strongly aggressive. In contrast to the other two forms, UV is not the main cause but rather a co-contributor among elderly or immunosuppressed patients (Lucas et al. 2019).

### 2.4.3. Vitamin D Production

Vitamin D production is the most commonly cited positive health effect of UVR. UVB radiation is absorbed by 7-dehydrocholesterol, resulting in the formation of first unstable pre-vitamin $D_3$ and subsequently stable vitamin $D_3$ (Holick 2001). The essential vitamin must be activated by two hydroxylations (introduction of hydroxyl to an organic compound): one in the liver and one in the kidneys (Lucas et al. 2019). Vitamin D's main relevance is its role in musculoskeletal health. Calcium and phosphorus absorption is only possible in presence of vitamin D and subsequently, blood calcium and phosphate levels are regulated by it. Low calcium levels (hypocalcaemia) can result in muscle weakness, cramps and fatigue. As calcium is essential for proper bone growth, severe cases of deficiency may lead to rickets and osteomalacia (soft bones) (Bikle, Adams, and Christakos 2018). Vitamin D has been associated with various other positive effects on health, however the causal mechanisms remain controversial. These include reductions in cancer mortality, reduced blood pressure, and reduced risks for multiple sclerosis, colorectal cancer, diabetes, and depression (Lucas et al. 2006; 2019). While supplementation of vitamin D carries risks that reach as far as toxicity in the form of calcium build-ups in the body (National Institutes of Healt Office of Dietary Supplements 2023), vitamin D-intoxication cannot occur from UV exposure because vitamin D synthesis only occurs until saturation (Holick 2001).

# 3. Research Question

The literature suggests that the Sun may enter a new modern grand solar minimum within this century. Grand solar minima are associated with reduced solar activity, which in turn cause lower levels of ozone production. Since stratospheric ozone is essential for absorbing UVR, the consequence is a paradox effect: lower solar activity leads to more UVR reaching the Earth's surface. As discussed, UV has several important health effects for humans. This merits the question: How will a potential grand solar minimum in the 21st century impact erythema, DNA damage and vitamin D production in humans?

To answer this question, the three health effects need to be made measurable in the form of erythemal, DNA damage and vitamin D radiation doses. This process is explained in more detail in chapter 4. Given the effects of a GSMi on ozone production and the role of ozone in regulating the amount of UV radiation that passes to the Earth described in chapter 2, three distinct predictions can be logically deduced:

1. A future GSMi will lead to an increase in erythemal, DNA damage and vitamin D radiation doses due to lower levels of stratospheric ozone formation resulting from reduced oxygen photolysis.
2. The strongest difference between a REF and GSMi future will occur in the midlatitudes due to the deceleration of polar vortices and the subsequent increased transport of ozone-rich air to the poles.
3. The difference between a REF and GSMi future will be more pronounced in the northern compared to the southern hemisphere due to the BDC-deceleration which affects the North more than the South.

# 4. Methods

Answering the research question requires defining erythema, DNA damage and vitamin D production in humans as measurable quantities. This can be done using radiation doses, which describe the estimated UV levels that cause erythema, DNA damage or vitamin D production. Radiation doses are derived by weighting UV irradiance at the ground by the spectral action spectra of the three health effects. As a reminder, an action spectrum describes the effect of radiation in eliciting a certain biological reaction (Urbach 2001; TEMIS and Royal Netherlands Meteorological Institute 2022). The computation of these radiation doses for potential future solar minimum conditions requires several steps that will be explained in more detail in the rest of the chapter.

1. Future atmospheric conditions for altered solar forcings need to be modelled using a coupled chemistry-climate and ocean model.
2. These conditions must then be used to compute solar radiation at the surface for different levels of solar activity using a radiative transfer model.
3. The predicted future solar radiation at the surface can then be used to calculate radiation doses by weighting with the respective action spectra.

The libRadtran software package was used to compute solar irradiance for different solar activity levels. It contains various tools to perform radiative transfer calculations in the Earth's atmosphere (Mayer and Kylling 2005). Radiative transfer refers to the absorption, scattering, and emission of radiation by atmospheric gases, aerosols, and clouds (Stamnes, Thomas, and Stamnes 2017). The software's main tool – the high-resolution *uvspec* radiative transfer model – was used for this thesis. It "calculates the radiation field in the Earth's atmosphere for a variety of atmospheric conditions" and has proven to be highly accurate (Mayer and Kylling 2005, 1855). *Uvspec* consists of several key components. The atmospheric state contains the input information on trace gas profiles, cloud liquid water content, cloud droplet size, and aerosol concentration profiles. These are then converted into optical properties by user-selected parametrizations. In the next part, the radiative transfer equation solver computes radiances, irradiances, and actinic fluxes based on the provided optical properties. Finally, the output is post-processed to receive output matching the units of the physical quantities (Emde et al. 2016). A schematic diagram of the model's structure can be seen in Figure 9.

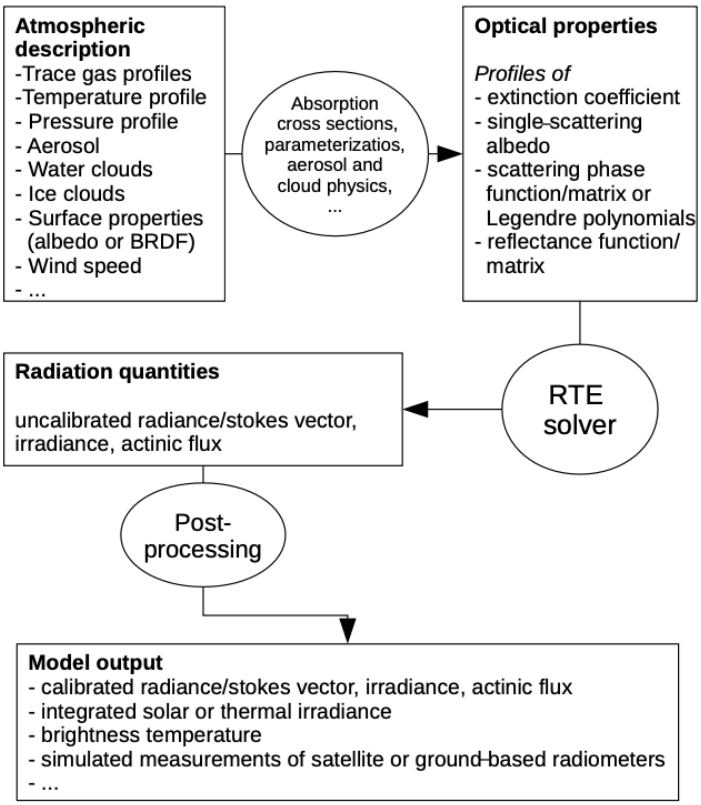


**Figure 9**: Figure 9: Radiative Transfer Model Structure (Emde et al. 2016, 1649)

The required climate model output was taken from the work of Arsenovic et al. (2018) on the implications of a grand solar minimum on climate and ozone layer. They used the coupled chemistry-climate and ocean model SOCOL3-MPIOM (Muthers et al. 2014) to simulate five different scenarios of solar forcing, each comprising two ensemble members. The reference scenario (REF) was simulated using a continued repetition of solar cycle 23 (1996-2008) until the year 2199. Two different strengths of minima were used in the other experiments based on the study of Anet et al. (2013): a strong drop (SD) where TSI was about 6.5 W $m^{-2}$ lower than in the reference scenario, and a weak drop (WD) where TSI was about 3.5 W $m^{-2}$ lower than in the reference scenario. For both these drops two different durations were simulated. The drops either continue throughout the 22$^{nd}$ century or start to recover after reaching their respective TSI minima around the year 2087 (SDR and WDR). This corresponds to a decrease in the 180–250 nm waveband of approximately 9% in the weak drop scenarios and 15% in the strong drop scenarios. For the non-recovery scenarios, the last solar cycle of both drop scenarios was repeated until the year 2199. The total solar irradiance change relative to the reference scenario is represented in Figure 10.

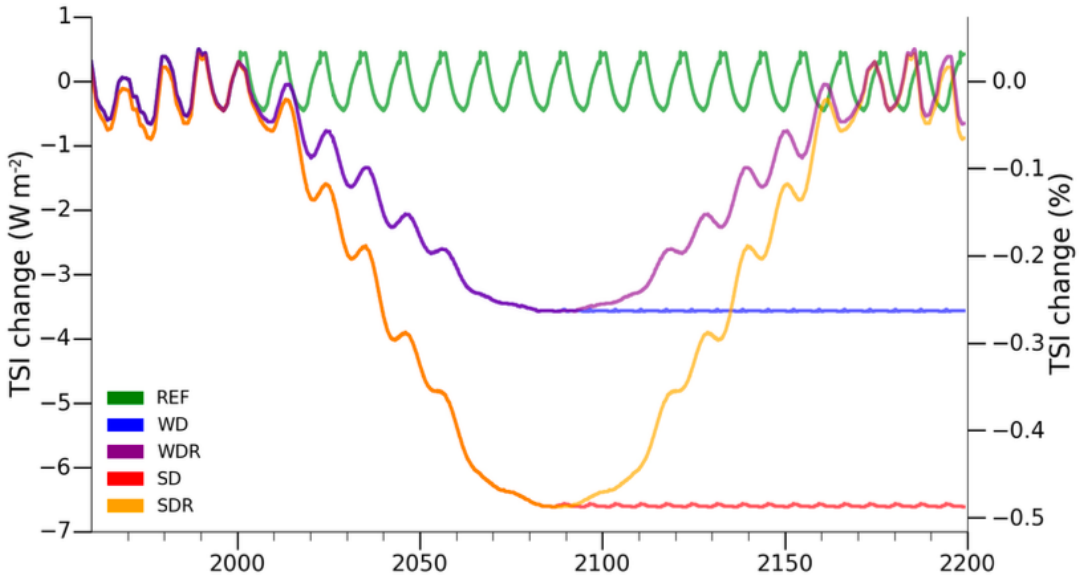


**Figure 10**: TSI change under different grand solar minimum scenarios (Arsenovic et al. 2018, 3472)

The simulations also followed Representative Concentration Pathway 4.5 (RCP4.5) RCPs describe different climate change trajectories predicting future atmospheric greenhouse gas concentrations based on varying human activity. They range from very high (RCP8.5) to very low (RCP2.6). RCP4.5 represents an intermediate pathway where policies and measures are implemented to mitigate greenhouse gas emissions, resulting in a radiative forcing level of 4.5 W/m² by the year 2100. Emissions are expected to peak in the 2040s and then decrease to stabilize at atmospheric $CO_2$ equivalent concentrations around 538 ppm by 2100. RCP4.5 foresees global mean temperature increase of 1.8°C and sea level rise of 0.47m between 2081 and 2100 (IPCC 2014).

The future atmospheric conditions predicted by Arsenovic et al. (2018) were then used as inputs for the libRadtran *uvspec* radiative transfer model to calculate surface direct spectral irradiance from 280-400 nm. Given the interest in impacts of UV on health effects in humans, information on ozone and $NO_x$ were of particular interest due to their UV-absorbing properties. As reduced solar irradiance leads to reduced NO photolysis which limits stratospheric $NO_x$ removal, higher stratospheric $NO_x$ levels are expected in the minimum scenarios: 10% more in case of SD and 5% more in case of a WD. Concerning ozone, both minimum scenarios would prevent a full ozone recovery within the simulated period compared to a recovery around mid-century. Due to the weaker polar

vortices caused by a reduction in solar activity, less ozone accumulates in the midlatitudes making them the most affected areas. Therefore, reduction in TOC may reach –20 DU in the midlatitudes compared to −10 DU in the tropics in SD. WD foresees a reduction of −5 DU. The change in total ozone column between 1960 and 2199 is displayed in Figure 11 taken from the authors.

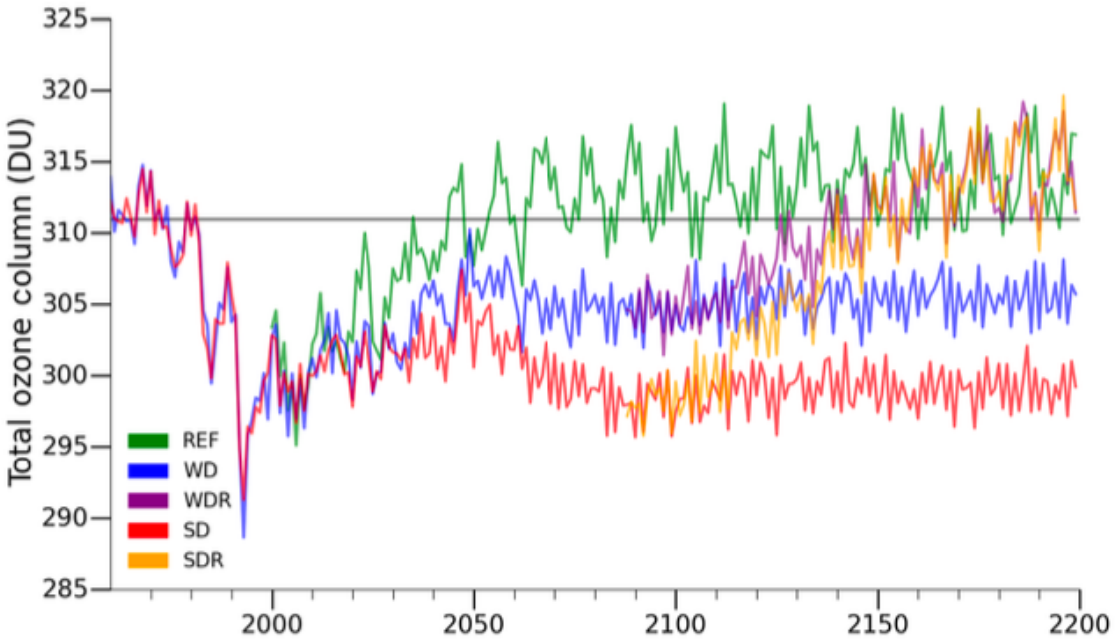


**Figure 11**: TOC change under different grand solar minimum scenarios (Arsenovic et al. 2018, 3479)

The output from the *uvspec* radiative transfer calculations is given as one value per wavelength band in mW/m$^2$/nm (Mayer and Kylling 2005). The irradiance dataset is a function of wavelength, latitude and time, so the dataset is organised into a three-dimensional array with axes corresponding to latitude, wavelength, and time. There are 25 wavelengths representing 25 wavelength bands, 48 latitudes ranging from -87 to +87, and 1200 time units representing months, corresponding to the monthly means between January 2100 and December 2199. This output was generated for the five different scenarios: reference (REF), strong drop (SD), strong drop recovery (SDR), weak drop (WD), and weak drop recovery (WDR). For all these scenarios, the onset of the GSMi begins around mid-century of the 21$^{st}$ century. For SDR and WDR it recovers around the same time in the 22$^{nd}$ century, while no recovery is expected for SD and WD.

Each of the experiments is composed of two ensemble members, i.e. slightly different but realistic initial conditions. To calculate the radiation health effects – erythema, DNA damage, and vitamin D production – radiation doses action spectra must be considered. As mentioned before, action spectra are a measure for the effectivity of wavelengths in eliciting a biological response (Urbach 2001). All three health effects have different action spectra, which were compiled by the Tropospheric Emission Monitoring Internet Service (TEMIS) based on the work of Webb et al. (2011), Bouillon et al. (2006), Setlow (1974), and Bernhard et al. (1997). The entire action spectrum data at 0.1 nm interval can be found at the Tropospheric Emission Monitoring Internet Service (TEMIS) of the European Space Agency (ESA) and the Royal Netherlands Meteorological Institute (KNMI)[1]. The graphical representation in Figure 12 shows the erythemal action spectrum covering UVA and UVB while the action spectrum of DNA covers mostly UVB, and the vitamin D action spectrum covers only UVB.

Applying these action spectra to the *uvspec* output necessitates coarsening of the action spectra because they are not compatible as such. The TEMIS-data is given at 0.1 nm intervals while the *uvspec* output consists of one value per wavelength band (5 nm), which would imply 50 action spectrum values for every wavelength band. Weighting the solar radiation with the relevant action spectra however requires one action spectrum value per wavelength band. To achieve this, the means of the action spectra data provided by TEMIS were calculated for each of the wavebands and indices respectively. The relevant boundaries can be found in Table 1. A new data frame using these coarsened values was created and is displayed in Table 1 as well as graphically in Figure 12, where the original action spectra can also be found. The coarsened action spectra clearly display the same patterns as the TEMIS-data. Both erythema and DNA damage show a high sensitivity to shorter wavelengths from 280-300 nm. Erythema decreases gradually, while DNA damage displays a very steep decline. The Vitamin D action spectrum demonstrates a different pattern with peak sensitivity between 290 and 305 nm. Between 300 and 305 nm this is even above erythema and DNA damage. Above 330 nm, vitamin D decreases significantly more rapidly than the other two action spectra. The coarsened values (solid line) and original values (dashed line) in Figure 12 clearly follow the same pattern, even

[1] https://www.temis.nl/uvradiation/product/figs/action_v20.dat

though there are very slight variations. This indicates that no vital information was lost during the approximation.

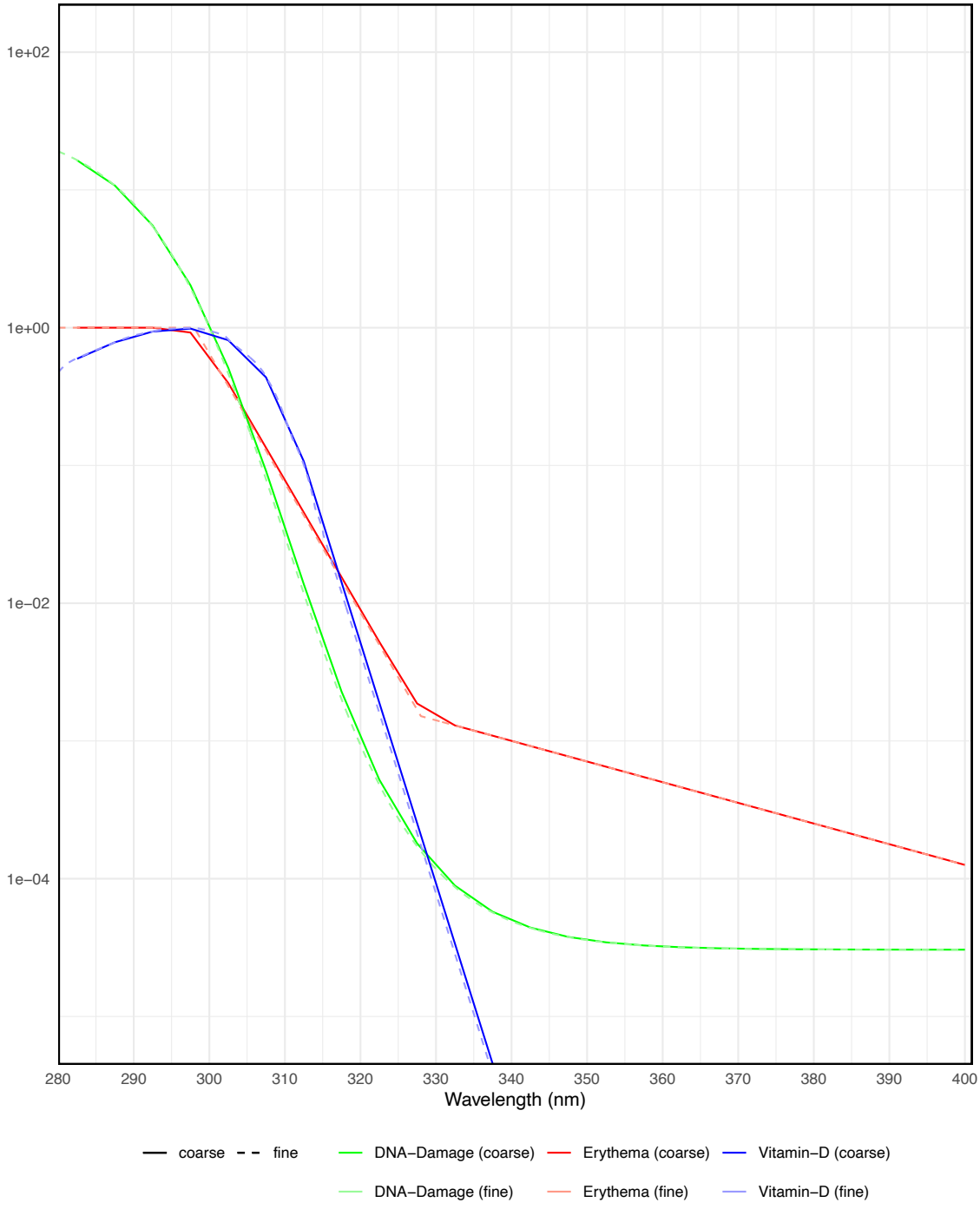


**Figure 12**: Original (dashed line) vs. Approximated (solid line) Action Spectra of Erythema, DNA Damage and Vitamin D Production

**Table 1**: Action Spectra per Waveband

| *Wavebands (nm)* | *Erythema* | *DNA Damage* | *Vitamin D* |
|---|---|---|---|
| 280-285 | 1 | 16.42219 | 0.5950297 |
| 285-290 | 1 | 10.76102 | 0.7836963 |
| 290-295 | 1 | 5.518879 | 0.9377549 |
| 295-300 | 0.9227168627 | 2.034825 | 0.9856275 |
| 300-305 | 0.3970277451 | 0.5119791 | 0.8115193 |
| 305-310 | 0.1345305667 | 0.09139952 | 0.4362152 |
| 310-315 | 0.0455848922 | 0.01376102 | 0.1071959 |
| 315-320 | 0.0154461790 | 0.002281275 | 0.01416766 |
| 320-325 | 0.0052338465 | 0.0005230005 | 0.001891869 |
| 325-330 | 0.0018694053 | 0.0001802167 | 0.000253109 |
| 330-335 | 0.0012973625 | $8.915542 \cdot 10^{-5}$ | $3.386291 \cdot 10^{-5}$ |
| 335-340 | 0.0010915937 | $5.750525 \cdot 10^{-5}$ | $4.530449 \cdot 10^{-6}$ |
| 340-345 | 0.0009184617 | $4.417025 \cdot 10^{-5}$ | $6.061184 \cdot 10^{-7}$ |
| 345-350 | 0.0007727894 | $3.780756 \cdot 10^{-5}$ | $8.109132 \cdot 10^{-8}$ |
| 345-350 | 0.0006502211 | $3.453131 \cdot 10^{-5}$ | $1.084903 \cdot 10^{-8}$ |
| 355-360 | 0.0005470929 | $3.276610 \cdot 10^{-5}$ | $1.451469 \cdot 10^{-9}$ |
| 360-365 | 0.0004603213 | $3.178945 \cdot 10^{-5}$ | $1.941889 \cdot 10^{-10}$ |
| 365-370 | 0.0003873121 | $3.124070 \cdot 10^{-5}$ | $2.598013 \cdot 10^{-11}$ |
| 370-375 | 0.0003258826 | $3.092962 \cdot 10^{-5}$ | $3.475823 \cdot 10^{-12}$ |
| 375-380 | 0.0002741960 | $3.075237 \cdot 10^{-5}$ | $4.650229 \cdot 10^{-13}$ |
| 380-385 | 0.0002307071 | $3.065106 \cdot 10^{-5}$ | $6.221447 \cdot 10^{-14}$ |
| 385-390 | 0.0001941159 | $3.059309 \cdot 10^{-5}$ | $8.323531 \cdot 10^{-15}$ |
| 390-395 | 0.0001633282 | $3.055986 \cdot 10^{-5}$ | $1.113587 \cdot 10^{-15}$ |
| 395-400 | 0.0001374236 | $3.054080 \cdot 10^{-5}$ | $1.489846 \cdot 10^{-16}$ |
| 400-405 | 0.0001258930 | $3.053430 \cdot 10^{-5}$ | $4.599510 \cdot 10^{-17}$ |

Manipulating the action spectra into an analysis-suitable format allows weighting the radiation output by the action spectrum associated with each respective wavelength. To do this, subsets of the data were taken from the time dimension, with each time slice representing one month. Then, the weights derived from the action spectra were systematically applied to the latitudinal data of the corresponding wavelength. This operation was repeated for all wavelengths. The next step was aggregating the weighted radiation values across all wavelengths. As the radiation output is given in $mW/m^2/nm$ the aggregated results must first be multiplied with 5 nm because of the 5 nm spacing of the wavelength bands averaged in the previous step (see Table 1). Then, the results must

also be divided by 25 mW/m$^2$ to arrive at the dimensionless erythemal, DNA damage and vitamin D doses for each latitude where 1 unit corresponds to 25 mW/m$^2$.

$$DNA_{month,lat} = \sum_{i=1}^{25} \frac{(r_i \cdot d_i) \cdot 5\ nm}{25\ mW/m^2} \qquad VitD_{month,lat} = \sum_{i=1}^{25} \frac{(r_i \cdot v_i) \cdot 5\ nm}{25\ mW/m^2}$$

$$Ery_{month,lat} = \sum_{i=1}^{25} \frac{(r_i \cdot e_i) \cdot 5\ nm}{25\ mW/m^2}$$

where $d_i$ = DNA weighting of radiation $r_i$ for wavelength $i$
$v_i$ = Vitamin D weighting of radiation $r_i$ for wavelength $i$
$e_i$ = Erythemal weighting of radiation $r_i$ for wavelength $i$

Reproducing these calculations for all 1200 time slices and the five experiments with their two ensemble members results in a measure of the intensity of erythema, DNA damage and vitamin D production for all combinations of latitude and month from 2100-2199. For analysis, both ensemble members for each experiment were averaged to give one set of results for each experiment.

These computed radiation doses were then analysed in multiple ways to answer the research question and test the hypotheses using the programming language for statistical computing and data visualisation R©. The data was evaluated to determine absolute changes over latitude and time, as well as total, regional, annual and centurial relative differences.

# 5. Results

## 5.1. The Reference Scenario

Meaningful analysis necessitates measuring the impact of a grand solar minimum in relation to non-minimum conditions, i.e. the reference scenario (REF). Figures 13-15 depict the development of erythema, DNA damage, and vitamin D UV doses over latitude and time for the last 10 years of analysis (2190-2200) in REF. Both seasonal and regional variations are evident, with noticeable increases in the summer months of both hemispheres in all regions that reflect usual patterns of TSI-intensity.

For erythema, seasonal differences range from around 4.0 in winter and 5.8 in summer in the polar North. In the northern midlatitudes, values range from ca. 4.9 in winter to 6.2 in summer. In the tropics, the range extends from around 7.2 in winter to around 8.2 in summer. Winter and summer differences range from 4.8 to 6.5 in the southern midlatitudes and 5.5 to 6.5 in the polar South. For DNA damage, the trends are the same but with lower values. Winter to summer differences range from around 1.5 to 3.5 in the polar North, 2.5 to 3.8 in the northern midlatitudes, 4.5 to 5.6 in the tropics, 2.5 to 4.2 in the southern midlatitudes, and 3.2 to 4.0 in the polar South. Vitamin D production displays the same seasonal variation. The winter and summer differences range from around 7.0 to 11.0 in the polar North, 8.5 to 11.5 in the northern midlatitudes, 13.0 to 15.5 in the tropics, 9.0 to 12.5 in the southern midlatitudes, and 10.5 and 11.5 in the polar South.

While all three effects are strongest in the tropics, clear differences can be seen between the northern and southern hemisphere. In the NH, there is a clear decrease in effect-intensity during the winter months that extends from polar- to midlatitudes. This is shown by the persistently lower values for all three effects in these regions, as well as the similarity of ranges in polar and midlatitudes in the NH (see above). In the summer months, intensity increases considerably, with slightly higher increases in the highest polar latitudes and lowest NH-midlatitudes. This effect is substantially more pronounced in the South. Not only are all three health effects stronger in the SH, but here, the polar region also undergoes higher intensities than the midlatitudes. This can be illustrated using regional index means: 5.8 for erythema, 3.4 for DNA damage, and 10.9 for vitamin D production in the SH midlatitudes. In the polar South mean doses were 6.0 for erythema, 3.8 for DNA damage, and 11.4 for vitamin D production. In contrast to the NH,

the pronounced decrease in the winter months is constrained within the midlatitudes, as shown by the greater differences between winter and summer months in the midlatitudes compared to the polar regions (0.7 units more for erythema, 0.9 units for DNA damage, and 2.5 units for vitamin D production).

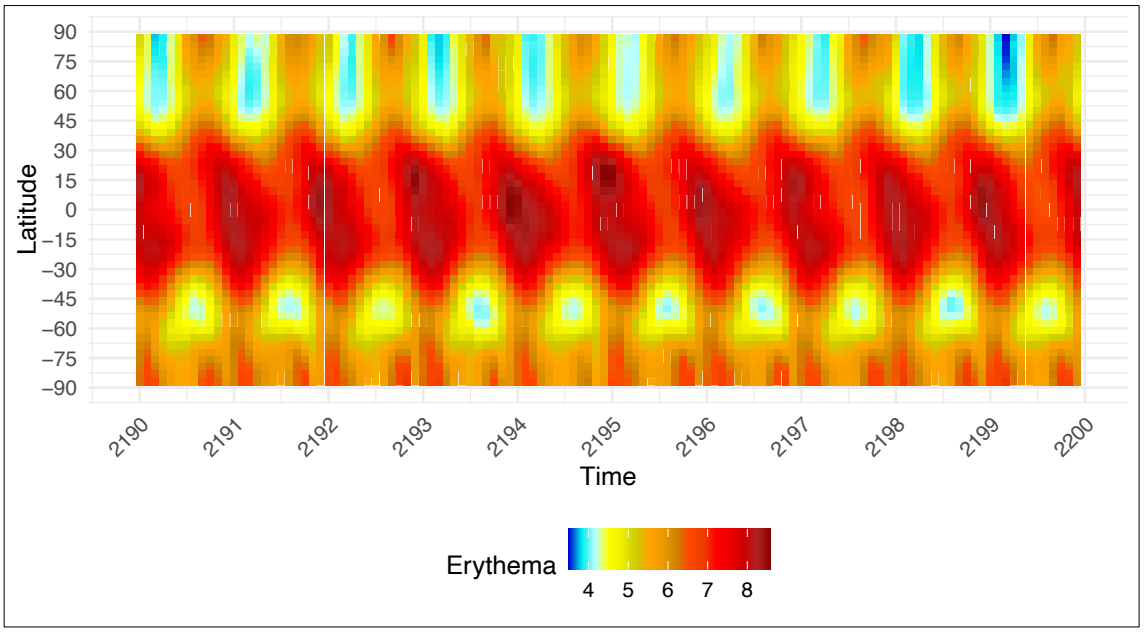


**Figure 13**: Spatial distribution of erythema in REF 2190-2200

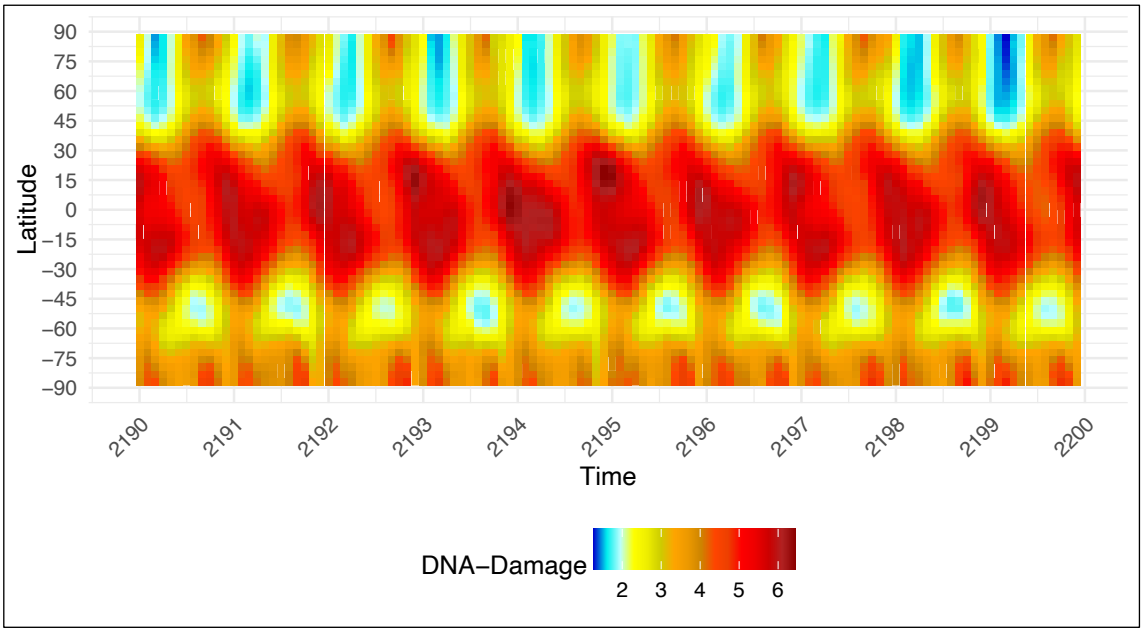


**Figure 14**: Spatial distribution of DNA damage in REF 2190-2200

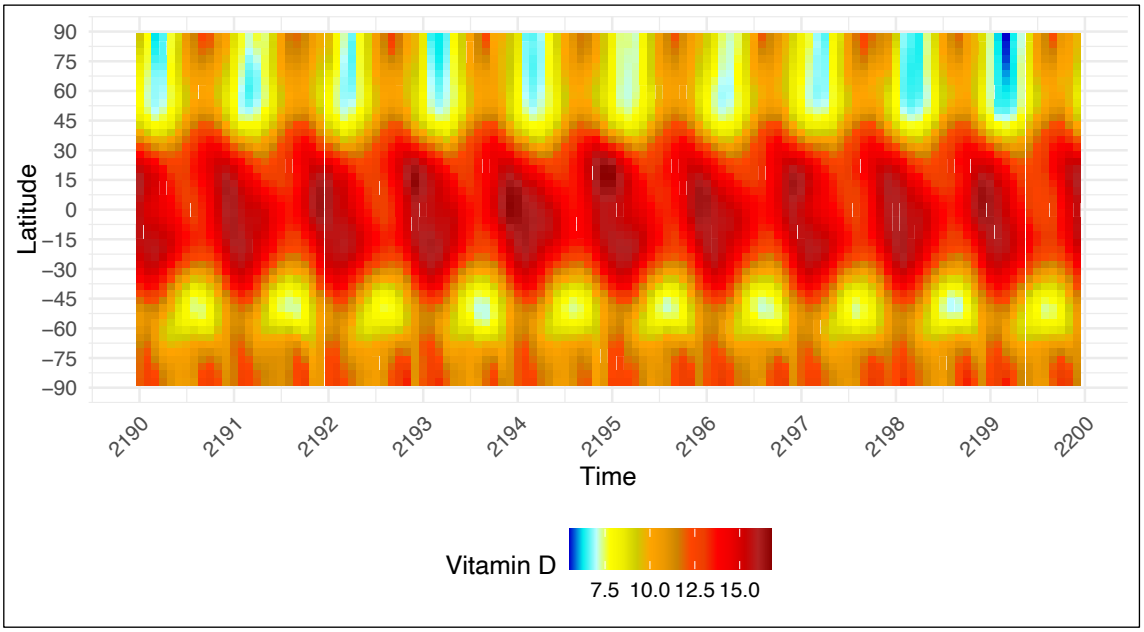


**Figure 15**: Spatial distribution of vitamin D production in REF 2190-2200

## 5.2. Global Annual Variation

To assess absolute change over time, global annual means for each of the effects were conducted over the entire simulated period and are represented in figures 16-18. The perpetuity of the 11-year solar cycle is distinctly detectable. Overall, vitamin D production exhibits the highest values, ranging around 11.5. This is followed by erythema ranging around 6.1, and finally DNA damage, which ranges around 3.8. We can also clearly see that in both SD and WD, all three health effects display a stronger intensity. WD is significantly below SD for all three health effects, however the difference between them is less pronounced for erythema than for DNA damage and vitamin D production. The difference between REF and SD is strongest for DNA damage, followed by vitamin D production and erythema. For the recovery scenarios (SDR and WDR) there is a substantial reduction in intensity around mid-century. For all three cases, SDR and WDR begin at approximately the same level as their respective SD and WD counterparts at the beginning of the century and end at approximately the same level as their respective REF counterparts at the end of the century. Another interesting observation is the difference in ranges of annual variation between the reference and drop scenarios. For all three, the range of annual and decadal variation is substantially greater in REF compared to SD and WD. This is attributable to the weakening of the solar cycle during GSMi described in chapter 2.1 and follows the same pattern as in past GSMi as illustrated in Figure 2 and 3.

In SDR and WDR, the SC becomes more pronounced after 2150, further indicating the recovery of usual solar activity.

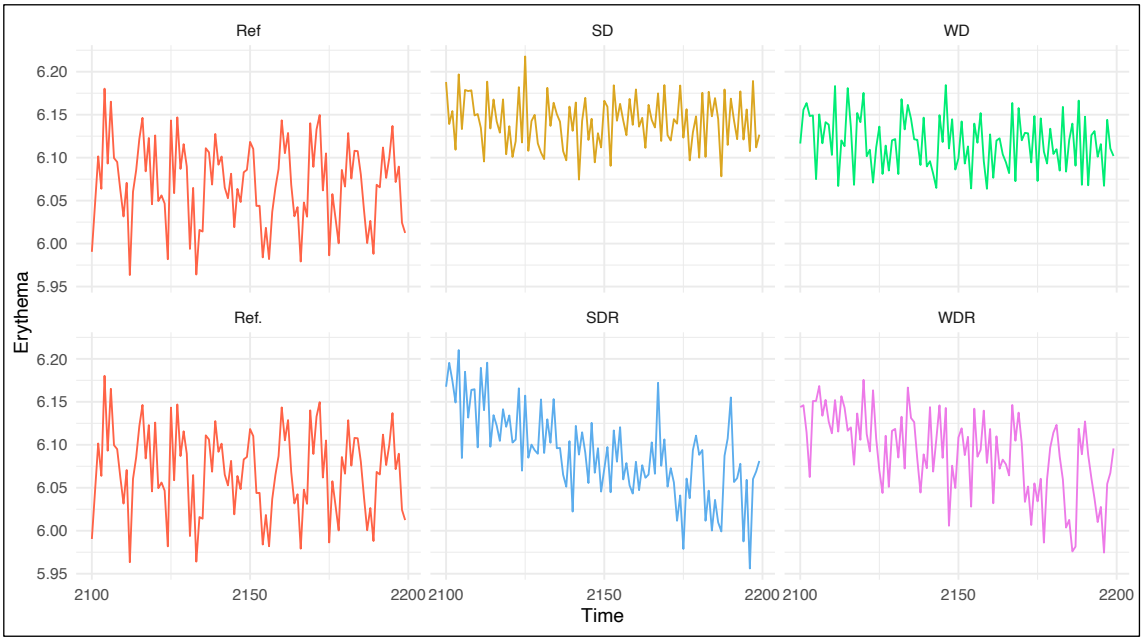


**Figure 16**: Global annual means of erythema for different grand solar minimum scenarios 2100-2200

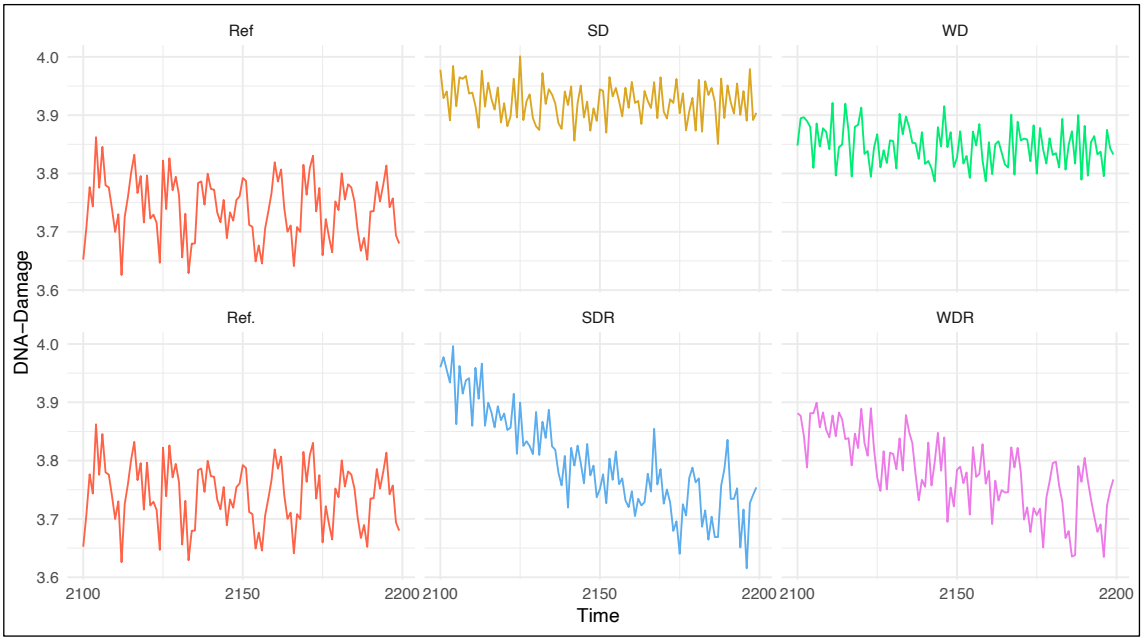


**Figure 17**: Global annual means of DNA damage for different grand solar minimum scenarios 2100-2200

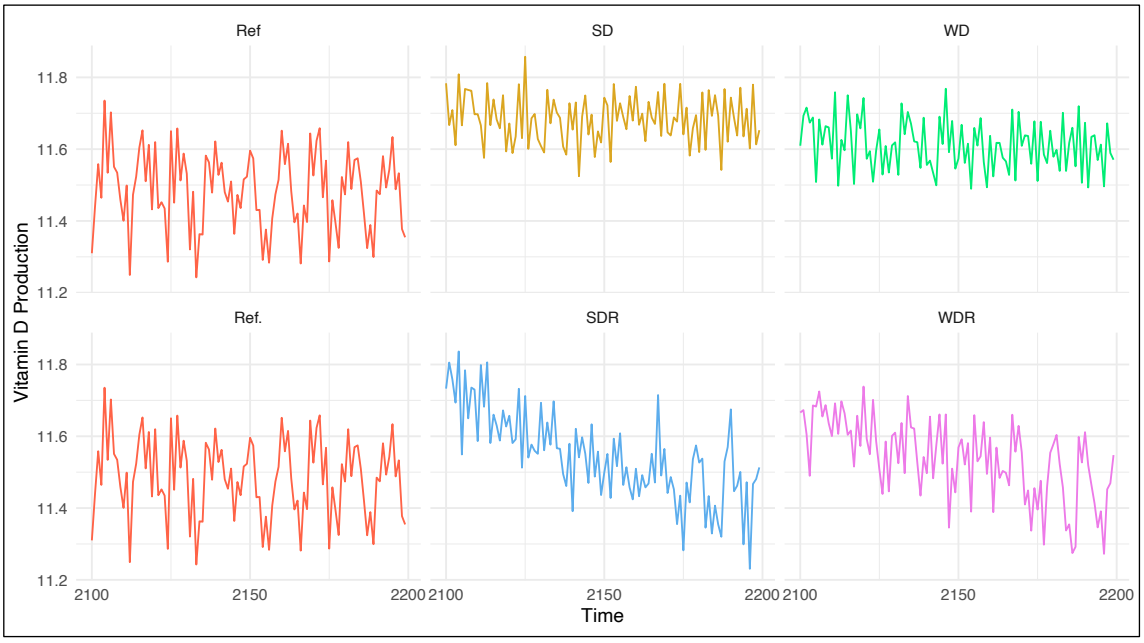


**Figure 18**: Global annual means of vitamin D production for different grand solar minimum scenarios 2100-2200

## 5.3. Development over Time

The annual means described in chapter 5.2. clearly depict both change over time and change from REF. Figures 19-21 allow further analysis of these changes by showing their magnitude for all three health effects. All scenarios follow the same annual pattern of divergence from REF albeit in varying strength. Some years display a strong positive change from REF of up to 3% for erythema, 9% for DNA damage and 4% for vitamin D production. Others display no change or even a slightly negative one down to -1.9% for erythema, -3.4% for DNA damage and -2.2% for vitamin D. This leads to outliers from the general pattern on an annual level but not concerning the overall trend (further discussed in chapter 5.4). These values also illustrate that the strongest change from REF occurs for DNA damage, followed by vitamin D production and finally erythema.

The development of the recovery scenarios is clearly visible, as WDR and SDR move from positive over no-change to negative relative change in relation to REF. After 2150, values are predominantly negative in WDR and SDR. This is exemplified by the difference in means for 2100-2150 and 2150-2200, where the latter are clearly below the former. For erythema, difference in means was −0.78% in SDR and −0.54% in WDR. For DNA damage, the respective change was −3.01% in SDR and −1.83% in WDR. For

vitamin D, −1.14% in SDR and −0.73% in WDR. Values in SD and WD remain predominantly positive, despite discernible differences between single years. This is displayed by the interquartile ranges, which in SD and WD respectively are 0.64-1.69% and 0.13-1.43% for erythema, 3.80-5.92% and 1.64-4.04% for DNA damage, and 1.05-2.39% and 0.32-1.84% for vitamin D. Additionally, differences in means between 2100-2150 and 2150 and 2200 were only marginal, showing the consistent trend over the entire time period: For erythema, difference in means were 0.2% in SD and 0.04% in WD. For DNA damage, 0.3% and 0.07%, and for vitamin D 0.2% and 0.007% respectively. Finally, the divergence from REF is stronger in SD than in WD, as shown by the higher values in all three interquartile ranges for SD.

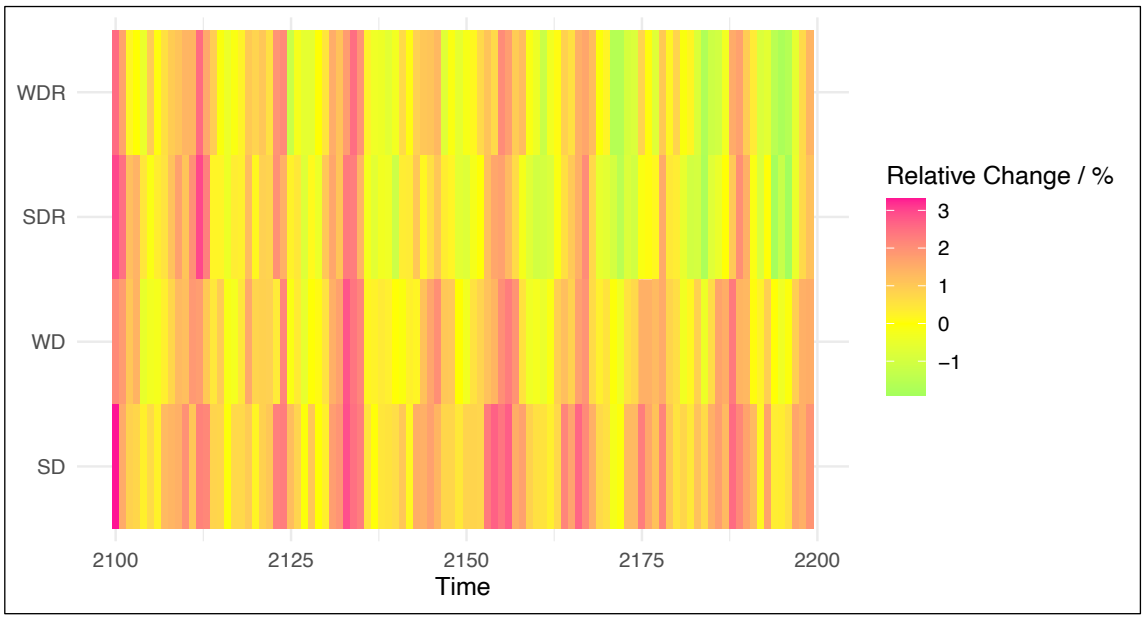


**Figure 19**: Relative change in erythema over time for different grand solar minimum scenarios

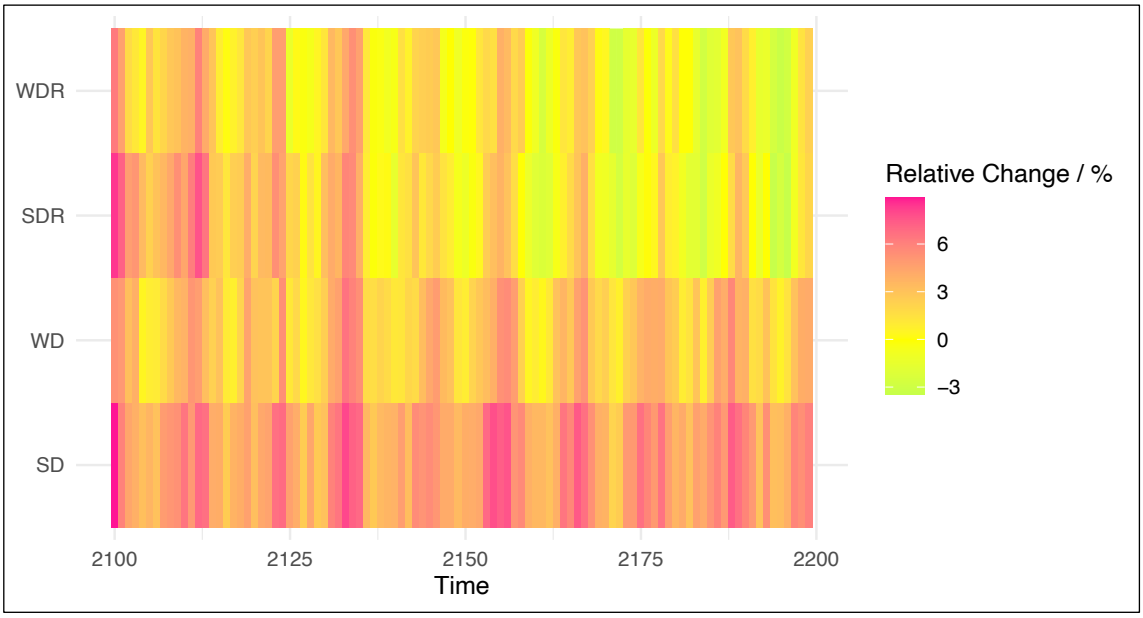


**Figure 20**: Relative change in DNA damage over time for different grand solar minimum scenarios

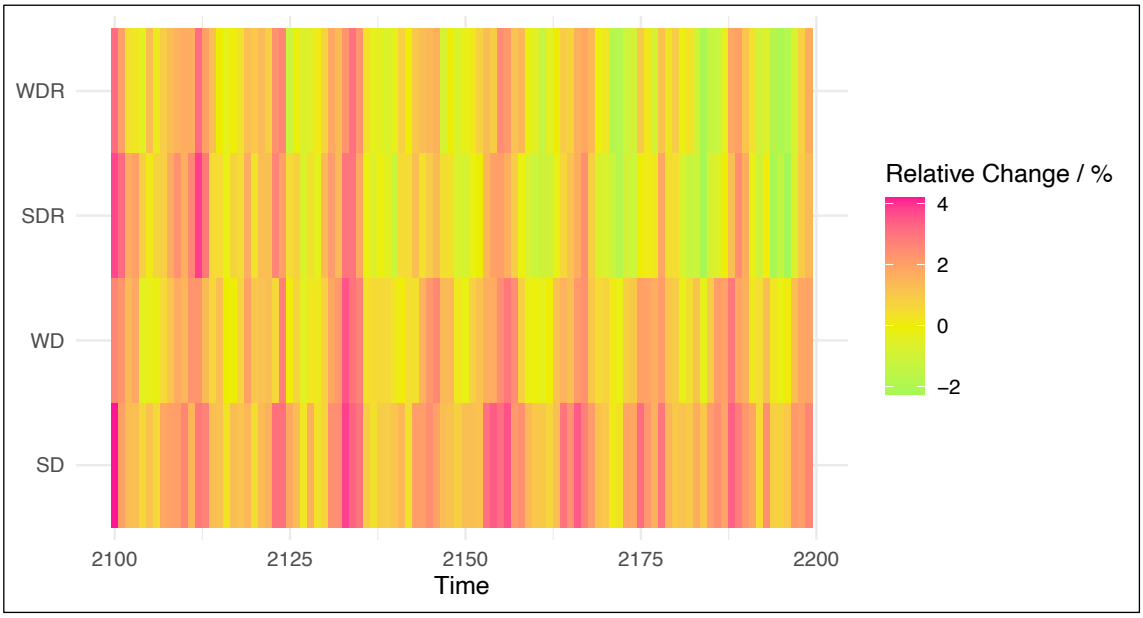


**Figure 21**: Relative change in vitamin D production over time for different grand solar minimum scenarios

As these results indicate, there is a distinct difference between end-of-century and beginning-of-century conditions for WDR and SDR. For WD and SD on the other hand, there is no apparent change. Therefore, these centurial differences are assessed further, with beginning-of-century defined as 2100-2120 and end-of-century as 2180-2200. The reference scenario shows a slight negative trend between beginning and end of century,

and this translates into WD, SD, WDR and SDR as well. However, as is intuitive from the discussed trends in the recovery changes, the difference between 2100-2120 and 2180-2200 are only statistically significant in SDR and WDR. This was tested using a two-tailed Student's t-test at 99% confidence interval. The magnitudes of the centurial change for the significant scenarios can be found in Table 2 as well as graphically in Figure 22, where centurial change is understood as ensemble means of the last 20 years minus ensemble means for the first 20 years in the simulated time period. The values reflect the changes relative to REF in order to exclude the overall negative trend between 2100 and 2200. Again, the strongest change occurs for DNA damage. The relative difference between WDR and SDR also follows this trend with the greatest difference pertaining to DNA damage, followed by vitamin D production and erythema.

**Table 2**: Ensemble means 2180-2200 minus ensemble means 2100-2120 relative to REF

| | *Erythema* | *DNA Damage* | *Vitamin D Production* |
|---|---|---|---|
| *SDR* | -1.36% | -4.62% | -1.88% |
| *WDR* | -1.00% | -2.94% | -1.33% |

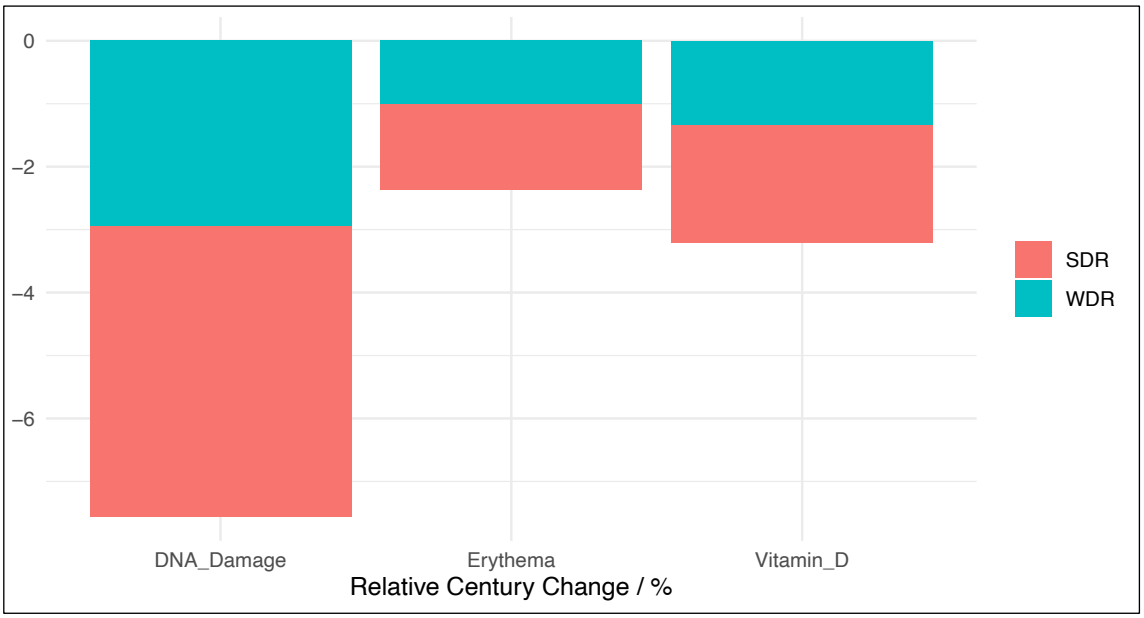


**Figure 22**: Ensemble means 2180-2200 minus ensemble means 2100-2120 relative to REF for a strong or weak drop in solar activity

## 5.4. Relative Change from Reference

In addition to comparing conditions at the end and beginning of the century, the overall change from the reference scenario should be considered as well. As has already become evident in the analysis, the relative difference for drop and REF conditions is strongest for DNA damage. SDR and WDR can be neglected in this analysis as they are ultimately identical to SD and WD in the first part of the century and identical to REF in the second part of the century. The relative differences from REF defined as the aggregated change between 2180-2200 for the three health effects are displayed in Table 3 and graphically in Figure 23. The relative difference between REF and both SD and WD are statistically significant at a 99% confidence interval as assessed using a two-tailed Student's t-test. The trends seen in the preceding results, namely the strongest relative change in DNA damage, followed by vitamin D production and erythema is confirmed by this test. The trend also extends to the relative difference between SD and WD

**Table 3**: Relative Change from REF 2180-2200

| | *Erythema* | *DNA Damage* | *Vitamin D Production* |
|---|---|---|---|
| *WD* | 0.718% | 2.73% | 1.03% |
| *SD* | 1.18% | 4.85% | 1.73% |

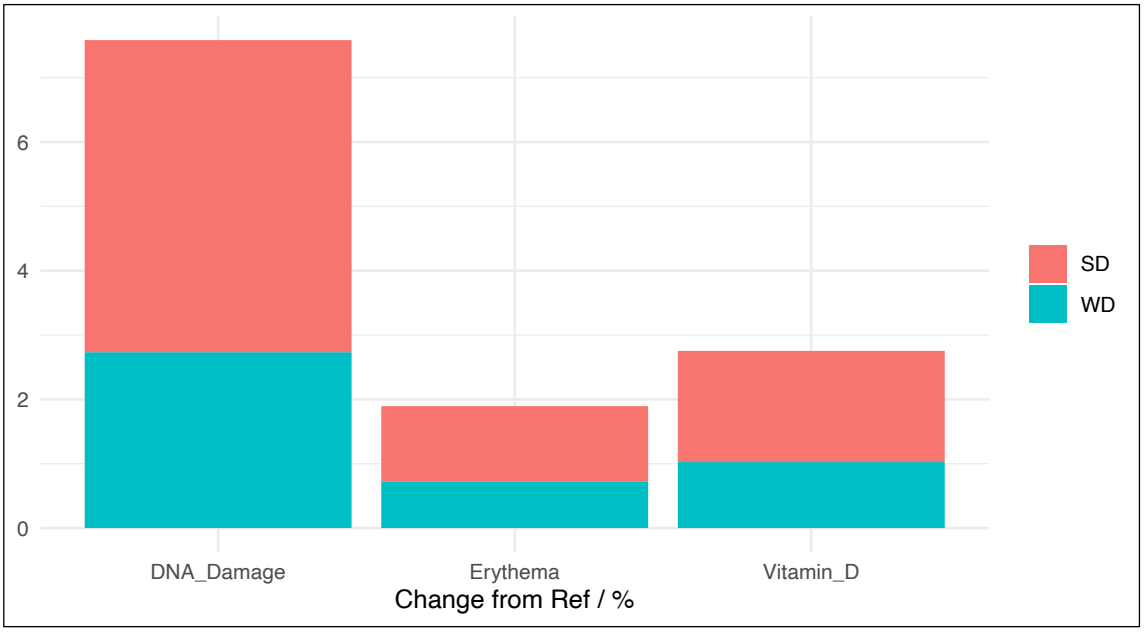


**Figure 23**: Total relative change from REF 2180-2200 for a strong or weak drop in solar activity

Relative change from REF also follows seasonal and annual trends. Figures 24–26 clearly show diverging activity according to summer and winter months but also persistently higher or lower activity during consecutive years reflecting the usual 11-year solar cycle. A LOESS (Locally Estimated Scatterplot Smoothing) was added to highlight the underlying trend of relative change from REF between 2190 and 2200. The smoothed trend line reveals a gradual decrease in intensity that reaches a minimum around winter 2195/2196, followed by a steeper increase in all three health effects. The local minimum likely reflects minimum solar activity within that particular Schwabe cycle. For erythema, relative change in SD decreases from around 1.7% in 2190 to 0.5% in 2196 and then increases to 2.4% end-of-century. In WD this development goes from 1% to 0% to 1.7% respectively. For DNA damage, the SD trend goes from around 6.0% to 3.1% and then 7.5%. For WD, from 3.0% to 1.25% and then 4.9%. For vitamin D production in SD the trend moves from around 2.5% to 1.0% to 2.9%. For WD, from 1.3% to 0.1% and then 2.5%.

Considerable variation exists pertaining to the relative difference from REF, as well as to the difference between the two drop scenarios. The highest change was observed in summer of 2194 with peak values around 3% for erythema, 9% for DNA damage, and 4% for vitamin D production. In some months, relative change from REF is even negative, which is likely attributable to the larger annual variance in REF (stronger solar cycle). For DNA damage, negative relative change only occurred in WD but for erythema and vitamin D negative change occurred in both WD and SD, likely because of the smaller magnitude of change between drop and reference scenarios. The strongest negative difference occurred in the winter months of 2191/2192 in WD with changes up to −1.7% for erythema, −2% for DNA damage, and −1.5% for vitamin D. Furthermore, WD overtakes SD in some months. This is likely caused by underlying changes in atmospheric composition that vary slightly over time between the scenarios. Nonetheless, SD is clearly stronger than WD overall, as can be seen from the smoothed conditional mean line. For erythema the difference between WD and SD remains around 0.7% until the winter months 2195/2196 and then decreases to around 0.5%. The same pattern occurs for DNA damage, with a change from around 3% to 1.8%. For vitamin D, the trend goes from 1.2% difference between WD and SD until 2195/2196, after which the difference is decreased to around 1%.

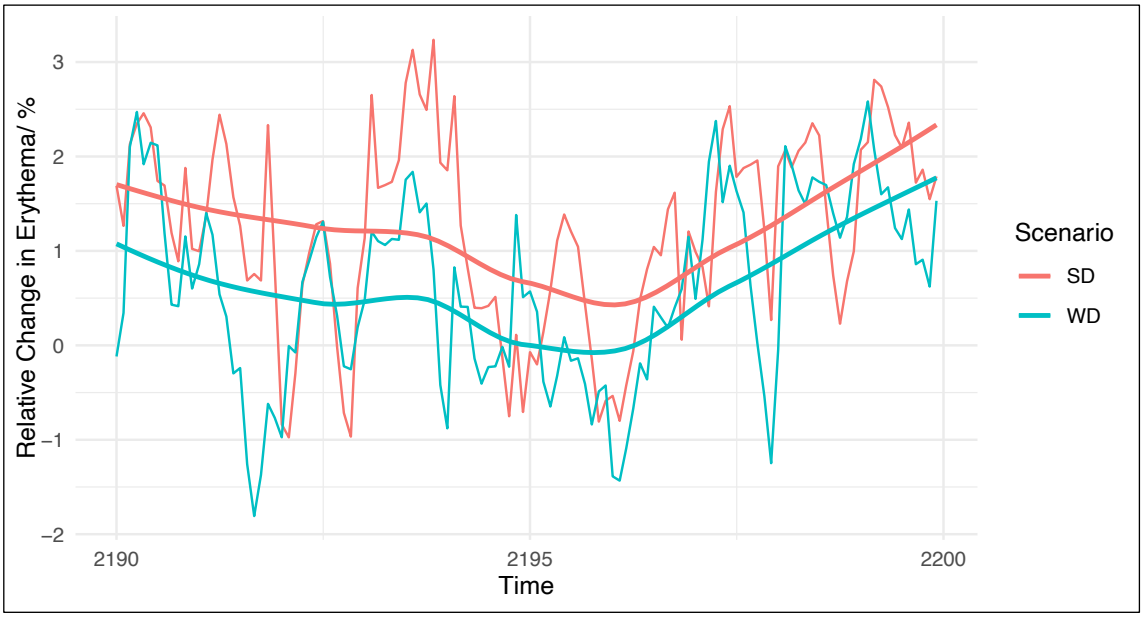


**Figure 24**: Relative monthly change in global erythema 2190-2200 for a strong or weak drop in solar activity including LOESS smoothing trend line

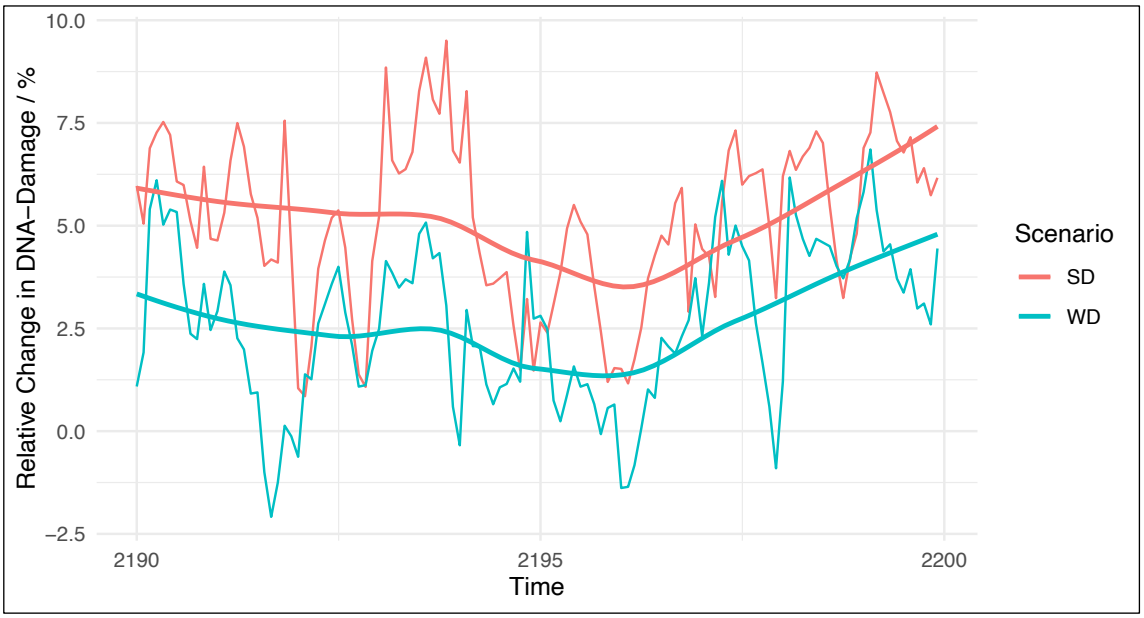


**Figure 25**: Relative monthly change in global DNA damage 2190-2200 for a strong or weak drop in solar activity including LOESS Smoothing Trend Line

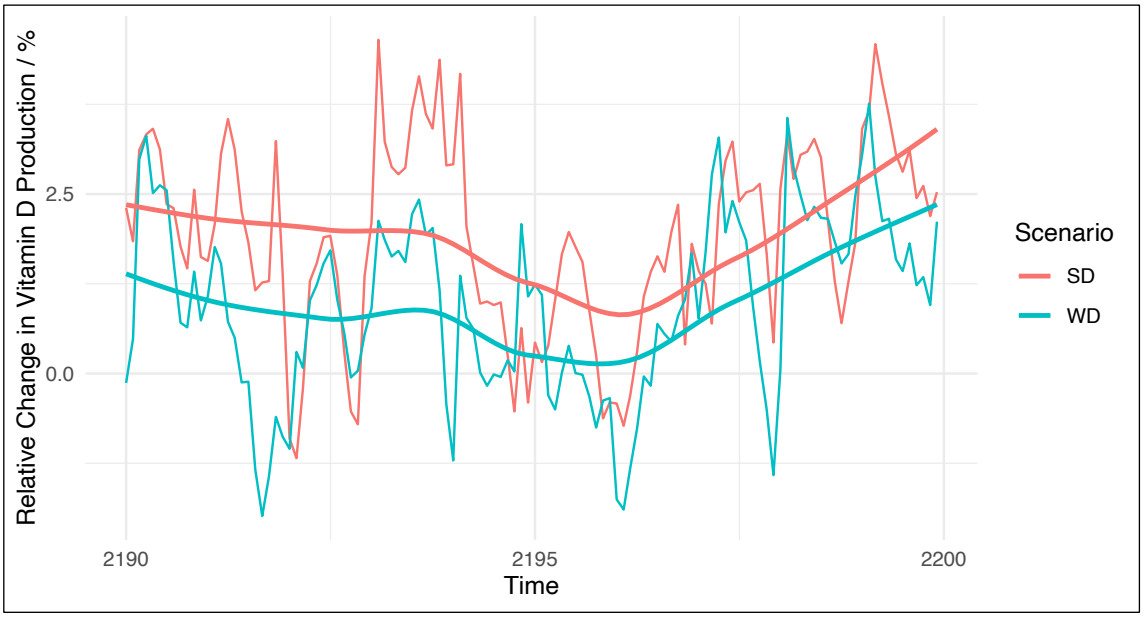


**Figure 26**: Relative monthly change in global vitamin D production 2190-2200 for a strong or weak drop in solar activity including LOESS smoothing trend line

## 5.5. Regional Variation

Finally, regional variation in the change of erythema, DNA damage, and vitamin D production was also examined by assessing the latitudinal distribution of the relative change between reference and drop scenarios. Figures 27-29 can be interpretated by looking at the length of the bars which represent change from REF at a particular latitude, i.e. a longer bar indicates stronger relative difference at this latitude. Since all bars follow the same overall shape, the figures illustrate that both WD and SD exhibit similar regional patterns. The differences are more pronounced in SD for all three health effects as shown by the greater change in bar length from levels of high change to levels of low change. The smallest differences were observed in the southern polar and tropical regions, indicating a lower sensitivity to variations in solar irradiance in these areas. For erythema, change was lowest between 79°S and 87°S with −0.15% in WD and 0.9% in SD. In the tropics, between 20°N and 20°S, relative change ranged between 0.5% and 0.7% in both WD and SD. This shows regional variation between WD and SD as change was lowest in the polar South for WD but in SD, it was lowest in the tropics. The same pattern occurred for DNA damage and vitamin D production. For DNA damage, change between 79°S and 87°S was 1.1% in WD and 4.5% in SD. Between 20°N and 20°S, relative change ranged around 3.6-3.9% in WD and 2.4-2.7% in SD. For vitamin D, relative change

between 79°S and 87°S was approximately 0.05% in WD and 1.25% in SD. Between 20°N and 20°S, values ranged 0.7% and 0.9% change in both WD and SD,

Conversely, the strongest changes were noted in the midlatitudes, suggesting a higher impact of reduced solar activity in these regions. Overall, the changes were more significant in the northern hemisphere compared to the southern hemisphere. For erythema, maximum change in the NH was 2.12% (at 46°N) in SD and 1.26% (at 39°N) in WD. Compared to this, maximum change in the SH was 1.67% (at 46°S) in SD and 1.13% (at 43°S) in WD. For DNA damage, maximum change in the NH was 6.90% (at 46°N) in SD and 3.82% (at 39°N) in WD. In comparison, maximum change in the SH was 5.92% (at 46°S) in SD and 3.56% (at 46°S) in WD. For vitamin D, maximum change in the NH was 3.44% (at 54°N) in SD and 1.83% (at 43°N) in WD. Compared to this, maximum change in the SH was 2.72% (at 50°S) in SD and 1.71% (at 46°S) in WD. Interestingly, for erythema and vitamin D production, the change was slightly negative in the lowest latitudes in WD, which could imply practically negligible influence of reduced solar activity on ozone recovery in these latitudes. The strongest regional change was observed between northern midlatitudes and tropics in SD for DNA damage with a difference of 3.29%. For erythema and vitamin D production, these regional differences were at 1.61% and 2.76% respectively.

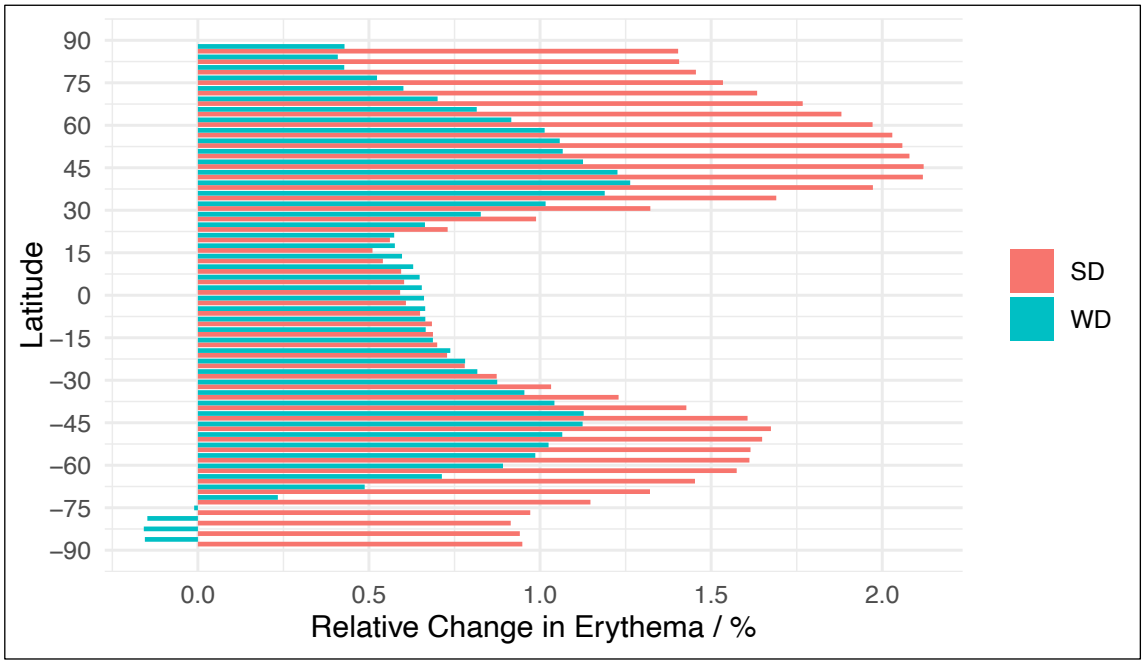


**Figure 27**: Latitudinal distribution of relative change in erythema 2180-2200 for a strong or weak drop in solar activity

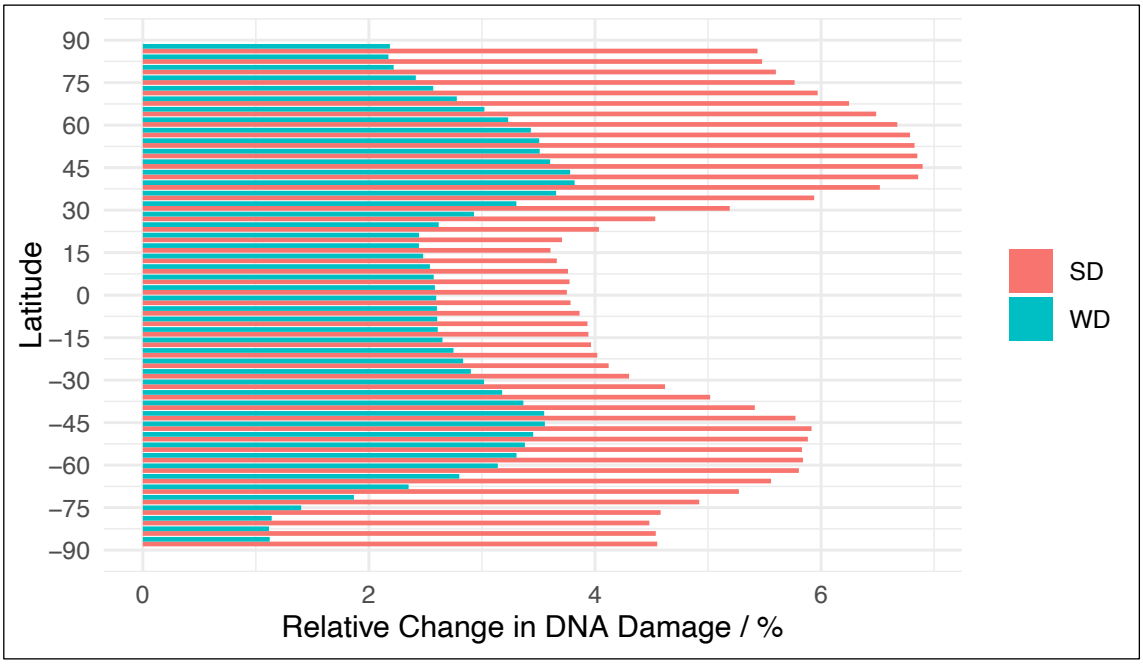


**Figure 28**: Latitudinal distribution of relative change in DNA damage 2180-2200 for a strong or weak drop in solar activity

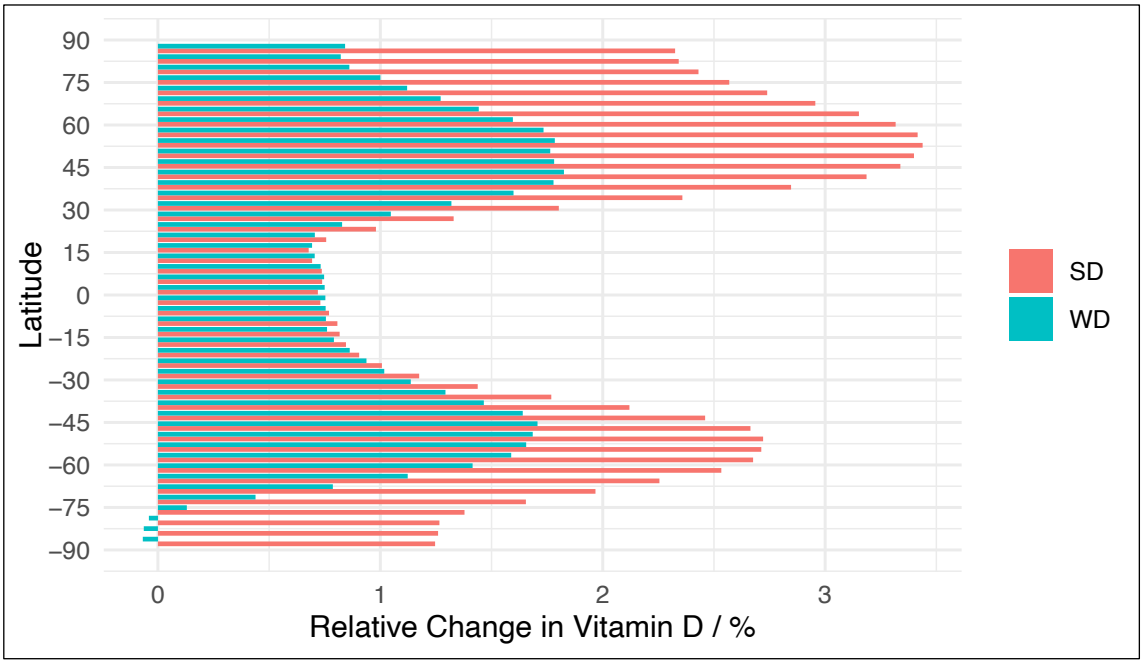


**Figure 29**: Latitudinal distribution of relative change in vitamin D production 2180-2200 for a strong or weak drop in solar activity

# 6. Conclusions and Outlook

## 6.1. New findings in the light of previous research

The results described in chapter 5 indicate a significant increase in erythemal, DNA damage and vitamin indices under GSMi conditions, regardless of the weakness or strength of the emerging minimum. In the recovery scenarios, the GSMi causes an increase that is sustained until approximately mid-century. The results thus corroborate the expectations deduced from previous research (Arsenovic et al. 2018): that increased UV radiation resulting from reduced solar activity and the subsequent decrease in stratospheric ozone leads to higher occurrences of erythema, DNA damage, and vitamin D production in humans, or rather that these effects occur at lower levels of exposure. These new findings will now be discussed in more detail and analysed in comparison to previous research.

All three health effects followed the same trends in the various analyses performed, albeit at different magnitudes. In absolute terms, UV doses are highest for vitamin D production, followed by erythemal and finally DNA damage. In SD, global mean vitamin D index ranged between 10-12 with maximum levels up to 16. Global mean erythemal index ranged between 5.5-6.5 with maximum levels up to 8.5, and global mean DNA damage index in SD ranged between 3-4 with maximum levels up to 7. This hierarchy reflects the same order of magnitude as current data on erythemal, DNA damage and vitamin D UV doses and is thus considered valid (see, e.g., Van Geffen et al. 2017 at https://www.temis.nl/uvradiation/UVarchive.php). However, this hierarchy is overturned when considering relative changes. For erythema, a weak drop of solar activity leads to a 0.72% increase in UV dose, while a strong drop causes a 1.18% increase. For DNA damage the values are 2.73% and 4.85% and for vitamin D production 1.03% and 1.73% respectively. These relative changes are averaged trends; however, relative change can reach peak values around 3% for erythema, 9% for DNA damage, and 4% for vitamin D production in certain months. These results confirm expectation 1 from chapter 3: A future GSMi will lead to an increase in erythemal, DNA damage and vitamin D radiation doses. Furthermore, they show that the impact of a GSMi is greatest on the DNA damage index. The difference between WD and SD is also most pronounced for DNA damage, emphasising its sensitivity. In the future, DNA damage UV doses should thus be monitored most thoroughly.

The development of UV doses over time described in chapter 5.2. and 5.3. also follows the trends expected from the literature. Both WDR and SDR showed statistically significant negative differences between the end and beginning of century. In SDR, ensemble means between 2180-2200 minus 2100-2120 showed relative differences of −1.36% for erythema, −4.62% for DNA damage, and −1.88% for vitamin D. Additionally, means in SDR and WDR clearly decreased between 2100-2150 and 2150-2200. For SDR, these changes were −0.78% for erythema, −3.01% for DNA damage, and −1.83% for vitamin D production. This trend reflects the recovery of stratospheric ozone around mid-century simulated by Arsenovic et al. (2018). Furthermore, the parallelism of developments over time underscore that ozone levels are the causal factor in determining erythemal, DNA damage and vitamin D index change. The differences between beginning- and end-of-century values relative to REF allow additional inferences about the sensitivity of the different effects. They remain in the same hierarchy, where DNA damage exhibits the largest change between 2180-2200 and 2100-2200 (followed by vitamin D and erythema). Hence, the evidence that DNA damage is the most sensitive of the three is substantiated: It not only increases the most under solar minimum conditions but also decreases most significantly when the minimum subsides.

Regional variation in erythemal, DNA damage and vitamin D radiation doses, too, follow distinct patterns. In the reference scenario, described in chapter 5.1, the results clearly corroborate the projected development of TOC under REF conditions found in the literature (Austin and Wilson 2006; Shepherd 2008; Waugh 2009; Li, Stolarski, and Newman 2009). Doses for all three effects are most pronounced in the tropics reflecting the extra-tropical ozone recovery caused by acceleration of the BDC which transports ozone away from the tropics towards the midlatitudes. For erythema, tropical values range between 7.2 and 8.2, for DNA damage between 4.5 and 5.6, and for vitamin D between 13.0 and 15.5. Additionally, the polar regions display a higher risk for the three health effects than the midlatitudes, which corresponds to the effect of the polar vortices preventing mixing of ozone-rich air with polar air (Arsenovic et al. 2018). In the SH, the mean erythemal index in the polar region was 6.0 compared to 5.8 in the midlatitudes. The mean DNA damage index was 3.8 compared to 3.4, and the vitamin D index was 11.4 compared to 10.9 respectively. Nonetheless, other factors influencing ambient UVR levels and subsequently erythema, DNA damage, and vitamin D production play an important role. This ambiguity can be seen in the results for the southern hemisphere,

which show an overall higher impact of the health effects, even though ozone recovery is predicted to be larger in the NH than in the SH (Li, Stolarski, and Newman 2009). The cause for this pattern can likely be ascribed to higher TSI in the South. Furthermore, TSI is higher in the tropics, making it hard to determine whether the causal mechanism behind the high radiation doses is low ozone levels or high solar irradiance. In order to definitively ascribe the effects to the impact of reduced ozone levels, the difference of minimum to reference scenario must be considered.

In absolute terms, the overall latitudinal pattern of dose intensity remains the same as in REF for all health effects and scenarios (not shown), implying that differences in regional TSI outweigh the effect of differing ozone levels. When assessing latitudinal variation in relative differences from REF, this pattern however changes significantly in the way described in chapter 5.5. As expected from the literature, relative change is strongest in the midlatitudes (Anet, Muthers, et al. 2013; Anet, Rozanov, et al. 2013; Maycock et al. 2015; Arsenovic et al. 2018). In SD, relative changes up to 2.12% for erythema, 6.90% for DNA damage, and 3.44% for vitamin D production occurred in the midlatitudes. Moreover, the strongest regional change was observed between northern midlatitudes and tropics in SD: 3.29% for DNA damage, 1.61% for erythema, and 2.76% for vitamin D production. Prediction 2 can therefore be affirmed: The strongest difference between a REF and GSMi future will occur in the midlatitudes. This is because, while reduced oxygen photolysis occurs everywhere, the weakened polar vortices no longer prevent mixing as successfully and thus allow more ozone to reach the poles. Additionally, ozone production is reduced in the tropical lower stratosphere in a GSMi (Arsenovic et al. 2018).

In addition, the BDC decelerates in a GSMi as a result of lower ocean surface temperatures that originate from reduced solar radiation. Thus, ozone recovery expected in REF is offset in the northern hemisphere. This effect is also shown in the results that display relative change being more pronounced in the NH than in the SH. In SD, maximum change in the NH was 2.12% compared to 1.67% in the SH for erythema. For DNA damage, maximum change in the NH was 6.90% compared to 5.92% in the SH. For vitamin D, maximum change in the NH was 3.44% compared to 2.72% in the SH. These hemispheric differences also corroborate the expectation that GSMi-conditions have less impact in the South as TOC changes are driven mostly by stratospheric levels of ozone depleting substances (Zubov et al. 2013). Therefore, expectation 3 can be affirmed: The

difference between a REF and GSMi future will be more pronounced in the northern compared to the southern hemisphere.

## 6.2. Health risks in solar minimum: the role of the individual

The findings of this thesis carry important implications concerning UV-related health effects on a global level. As discussed in the literature review, cancer of the skin is the most abundant type of cancer worldwide. Under solar minimum conditions, adverse effects of UV would occur with higher intensity, meaning less exposure is necessary to cause erythema or damage to DNA. As both conditions are precursors for skin cancer, a correlating increase in cutaneous malignant melanoma, keratinocyte cancers, and Merkel cell carcinoma could be expected if no adaptation occurs. Quantitative deductions about the magnitude of increase in skin cancer are however impossible with the methods applied here. A possible indication could be the results of van Dijk et al. (2013) who calculated that two million cases of skin cancer per year have been prevented by the Montreal Protocol. Anthropogenic ozone depletion through ODSs however is substantially more pronounced than naturally induced ozone reductions expected during a GSMi. Hence, increases in skin cancer resulting from a solar minimum can be expected to be considerably below the estimate of two million additional cases per year (keeping in mind that 1.5 million new cases per year are diagnosed already today).

The strong increase in DNA damage in a possible GSMi should manifest an enhanced cause for concern, as skin cancer is directly caused by DNA damage, while erythema acts as an additional risk factor. Fortunately, adaptation is possible presuming access to sufficient information. In fact, UV exposure is highly individual and depends on personal behaviour and skin pigmentation as well as geographic location (Lucas et al. 2006; 2019). UV doses are contingent on time spent outdoors and personal protective measures, making generalisations about population groups difficult. Indeed, variance ranges between 0.1 and 10 times the mean. (Gies et al. 1999). Nonetheless, there are certain risk groups that generally experience higher exposure levels, namely males, outdoor workers, children and adolescents (Gies et al. 1999; Raymond-Lezman and Riskin 2023; Symanzik and John 2022). Skin pigmentation is another relevant factor, where deeply pigmented skin provides significant additional protection against UVR (Lucas et al. 2006).

These individual predispositions are especially relevant concerning the regional distribution of relative change under solar minimum conditions. Assuming there are no substantial changes in population patterns during the next century, the majority of inhabitants in the tropics has deeply pigmented skin. Thus, they have a better protective mechanism against UVR and live in areas with less changes in erythemal, DNA damage and vitamin D UV doses. The combination of individual factors and latitudinal patterns warrants the conclusion that adaptation will be most essential in the northern midlatitudes. The higher level of change observed here is further reinforced by the lower level of natural protection against UV at least among the majority of the population that is predominantly lightly pigmented. Intensification further occurs through the widely disseminated cultural practice of tanning and a presumable increase in exposure resulting from higher ambient temperatures in the future (Lucas et al. 2019). It is important to remember that overall doses will still be highest in the tropics due to higher irradiance. Yet, given that the change between GSMi and REF scenarios is not as pronounced, adaptation is less vital. Additionally, incidence of skin cancer is lower among predominantly deeply pigmented populations (Lucas et al. 2019).

The individual factor determining UVR exposure allows considerable potential for education-based adaptation. Actors such as the World Health Organization (WHO), national health agencies and national radiation agencies could play pivotal roles in educating citizens on the increased risk of UV exposure under solar minimum conditions. Such educational campaigns should stress the effectiveness of protective measures such as avoiding sun especially around solar noon, applying sunscreen, and wearing hats, sunglasses and skin-covering clothing, which have been shown to reduce exposure by 50-90% (Gies et al. 1999). As estimates suggest that 25-50% of UV exposure before the age of 60 arises during childhood (Raymond-Lezman and Riskin 2023), it is vital to provide and adjust UV literacy to these age groups. Advances in technology also provide opportunities, for example by incorporating information on UVR into weather forecasting applications.

Nonetheless, research suggests that health promotion programs only have a limited effect. Numerous studies show that people deliberately expose themselves to the sun despite being aware of the risks – especially among light-skinned populations (Lucas et al. 2014; Satagopan et al. 2015; Taylor, Westbrook, and Chang 2016; Gellén et al. 2016; Flannery

et al. 2016). Furthermore, sunburn remains a very common phenomenon regardless of risk-education. In the US National Health Interview Survey 2010, for example, 37% of adults reported at least one incidence of sunburn, with cases increasing for 18-29-year-olds (52%) and light-skinned respondents (44%) (Holman et al. 2014). In Hungary, as many as 74% of 12-19-year-olds reported at least one episode of serious sunburn. Especially indicative is the fact that even personal or family history of cutaneous malignant melanoma displays no effect on risk-taking behaviour concerning sun-exposure (Nahar et al. 2016; Glenn et al. 2015). It is difficult to assess the impact of awareness-building measures as there is no way to compare group samples with and without exposure to such measures from within the same population – the common dilemma of counterfactuals. Nonetheless, the evidence underscores that efforts to implement effective health protection measures need to be enhanced in a GSMi-scenario given the straightforward and practical prevention strategies available. This is especially true for the northern midlatitudes. A decrease in solar activity without adequate adaptation would not only increase the risk of serious health impairments for a large proportion of the world population but also impose immense costs on public health systems (Guy et al. 2015).

## 6.3. Health benefits in a solar minimum: striking a balance

Beneficial consequences of ultraviolet radiation also exist, the most important being Vitamin D production. It will remain important to strike a healthy balance between negative and positive UVR effects under future solar conditions. In contrast to erythema and DNA damage, increased UV doses cannot result in overproduction of vitamin D and its related harmful impacts on human health because of the biological saturation barrier (Holick 2001). Hence, GSMi-conditions entail positive impacts on human health given that more regions on Earth are supplied with enough UV for sufficient vitamin D production and no risks of overproduction exist. This would entail positive effects on muscle, tissue and bone health, as well as potentially other effects that require further research into causality (Bikle, Adams, and Christakos 2018) However, vitamin D production, erythema and DNA damage are inextricably linked. If the higher hazards of UV-induced harm provoke sun-avoiding behaviours, this would also reduce the health benefits from expected increase in vitamin D production. This counter-intuitive relationship could nevertheless be offset. First, while evading the sun or wearing

protective clothing completely blocks UV, there is little evidence to suggest that the use of sunscreen prohibits vitamin D production (Neale et al. 2019). Furthermore, absolute radiation doses are higher for vitamin D production than for erythema and DNA damage. Hence, less exposure is necessary to induce vitamin D production so that sun exposure that is both beneficial and safe could be possible. On the other hand, the impact of a potential grand solar minimum is greater on DNA damage than on vitamin D production. This means that negative effects of solar radiation are more pronounced during GSMi conditions compared to the reference scenario. It is difficult to predict how exactly a potential minimum would affect the balance between the three effects considering the high relevance of individual behaviour. Nonetheless, given the possibilities to safely supplement vitamin D it could be advisable to focus more on erythema and DNA damage in adaptation efforts.

## 6.4. Limitations

Despite the significant findings of this thesis, several limitations should be acknowledged to provide a comprehensive understanding of the results. First, the methodology is based on several assumptions made to simulate future conditions. Both SOCOL3-MPIOM and libRadtran are highly sensitive models but they cannot perfectly predict future atmospheric states or radiation doses. They rely on parametrisations of atmospheric processes, particularly the interactions between various trace gases and aerosols, which could result in model outputs that do not accurately capture real-world variability. For libRadtran for instance, clear-sky conditions were used as model inputs and thus the results do not depict interactions between solar radiation and clouds, despite numerous regions on Earth undergoing sustained periods of cloud cover. In this sense, the coarsening of action spectra data, while necessary for compatibility, might introduce some loss of detail and potential inaccuracies in assessing health effects. Likewise, the restriction of spatial resolution to latitude bands limits the potential to capture more localised effects.

Additionally, while the RCP4.5 assumed in the SOCOL3-MPIOM modelling is a moderate scenario, real-world emissions and policy changes might follow a different pathway, affecting atmospheric composition and subsequently radiative transfer. If substantial changes occur to anthropogenic behaviours within the next 50 years, these

results may no longer be accurate. Moreover, using only two ensemble members might not capture the full range of natural variability, leading to potential underestimation of uncertainty, because slight differences in initial conditions might lead to significant variations in long-term projections. And finally, the chosen TSI drops (weak and strong) are based on historical analogues and may not encompass the full range of possible future solar activity.

Besides modelling limitations, this research could have benefitted from a deeper analysis of the biological mechanisms underlying erythema, DNA damage and vitamin D production. Such an analysis would allow establishing more profound contextualisation within the existing literature on human health. While the results of this study successfully demonstrated that a grand solar minimum would significantly increase radiation doses of erythema, DNA damage and vitamin D production, no valid predictions can be made on the exact extent of impact on the biological effects affiliated to these three UV-related mechanisms. Such qualitative assessments would also allow deductions about the balance of positive and negative UV health effects in a grand solar minimum. However, these types of analyses would require profound biological or medical knowledge and thus exceed the possibilities within this thesis. Nevertheless, interdisciplinary approaches should be considered for further research.

## 6.5. Outlook

Future UVR exposure cannot be examined without addressing its complex interactions with climate change, especially concerning the role of individual behaviour and genetic predispositions in determining risk level. Warmer ambient temperatures can alter such attitudes, for instance by increasing time spent outside in cooler regions and reducing outdoor activities in hotter regions, especially around midday. Additionally, higher temperatures can decrease tendencies to wear protective clothing, thus increasing exposure (Lucas et al. 2019). Climate change also exerts other societal impacts, such as altering the structure of the labour market, which may lead to unforeseen health effects. For instance, the workforce employed in the renewable energy sector – which is expected to grow in the future – faces increased exposure to high levels of UV radiation (Samaniego-Rascón et al. 2019). These relationships could potentially counteract health protection measures and should be considered in a solar-minimum-future. Other indirect

health effects of climate-UV interactions include altered plant growing seasons that can impact allergic conditions in humans (Bornman et al. 2019), as well as changes in food quality and quantity through changes in atmospheric composition and air quality (Wilson et al. 2019).

Given the complex interactions of UVR, human and ecosystem health, the possibility of a grand solar minimum occurring in the next century is of great significance. Future research should investigate direct and indirect mechanisms. In particular, UV is harmful to the eye, increasing the risk for inflammation of the cornea (photokeratitis), invasive growths in the eye (pterygium), and increasing clouding of the lens (cataract) (Lucas et al. 2014; Chawda and Shinde 2022). Cataract is a primary cause of blindness and estimates suggest around 15 million people worldwide that are blind due to cataracts (WHO 2022). A logical hypothesis would thus be an increase in ocular UV index under GSMi-conditions. Increases in UVB levels have also been shown to negatively affect resiliency of disease-carrying insects, indicating a potential positive indirect health effect of increased UV because less pathogenic insects survive (Tetreau et al. 2014). Another positive effect might arise from UV's surface water-disinfecting properties, which could be especially relevant in light of potential future water scarcity (Williamson et al. 2019). On the other hand, UV is also very effective in breaking down pollutants, both organic and inorganic such as pesticides, fertilisers, pharmaceuticals, plastics and microplastics (Sulzberger et al. 2019; Andrady, Pandey, and Heikkilä 2019). Given the complexity of biogeochemical cycles, multiple feedback mechanisms might result in widespread environmental impacts. These include increases in the release of harmful gases from UV-induced degradation processes and eutrophication from higher photosynthetic activity (Sulzberger et al. 2019). Besides causing environmental damage, such processes – enhanced by higher UV in solar minimum conditions and its interactions with climate change – could impede human health directly through diminishing air quality or accumulation of harmful substances in the food chain, as well as indirectly through limiting ecosystems services.

Future research would benefit from building on the findings generated in this study. The understanding of the mechanisms underlying solar activity, UV radiation and human health could be enhanced by examining the development of radiation doses under other representative concentration pathways. This would enable inferences about the agency

humans have in averting impacts of the potential solar minimum on their health. Moreover, the findings could be used to quantify the skin cancer-risk posed by a weak or strong drop in solar activity. The global burden of disease from ultraviolet radiation would likely change in light of a future solar minimum. Thus, assessment would have to be renewed taking into account these new findings. Finally, this thesis provides the basis to develop updated guidelines concerning exposure to sunlight. As has been shown, these guidelines would be subject to variation concerning geographic location and individual predispositions. Again, the development of such recommendations would benefit from interdisciplinary expertise. Nonetheless, researchers and practitioners of UV-related biological health effects should be well equipped in adjusting the guidelines using the new findings presented here.

# List of References


Abdussamatov, H.I. 2016. 'The New Little Ice Age Has Started'. In Evidence-Based Climate Science, edited by Don J. Easterbrook, 307–28. Amsterdam; New York: Elsevier Science. https://doi.org/10.1016/B978-0-12-804588-6.00017-3.

Abreu, J. A., J. Beer, and A. Ferriz-Mas. 2010. 'Past and Future Solar Activity from Cosmogenic Radionuclides'. *ASP Conference Series* 428 (June):287–95.

Abreu, J. A., J. Beer, F. Steinhilber, S. M. Tobias, and N. O. Weiss. 2008. 'For How Long Will the Current Grand Maximum of Solar Activity Persist?' *Geophysical Research Letters* 35 (20): L20109. https://doi.org/10.1029/2008GL035442.

Andrady, A. L., K. K. Pandey, and A. M. Heikkilä. 2019. 'Interactive Effects of Solar UV Radiation and Climate Change on Material Damage'. *Photochemical & Photobiological Sciences* 18 (3): 804–25. https://doi.org/10.1039/c8pp90065e.

Anet, J. G., S. Muthers, E. Rozanov, C. C. Raible, T. Peter, A. Stenke, A. I. Shapiro, et al. 2013. 'Forcing of Stratospheric Chemistry and Dynamics during the Dalton Minimum'. *Atmospheric Chemistry and Physics* 13 (21): 10951–67. https://doi.org/10.5194/acp-13-10951-2013.

Anet, J. G., S. Muthers, E. V. Rozanov, C. C. Raible, A. Stenke, A. I. Shapiro, S. Brönnimann, et al. 2014. 'Impact of Solar versus Volcanic Activity Variations on Tropospheric Temperatures and Precipitation during the Dalton Minimum'. *Climate of the Past* 10 (3): 921–38. https://doi.org/10.5194/cp-10-921-2014.

Anet, J. G., E. V. Rozanov, S. Muthers, T. Peter, S. Brönnimann, F. Arfeuille, J. Beer, et al. 2013. 'Impact of a Potential 21st Century "Grand Solar Minimum" on Surface Temperatures and Stratospheric Ozone'. *Geophysical Research Letters* 40 (16): 4420–25. https://doi.org/10.1002/grl.50806.

Ansary, Tuba M., Md Razib Hossain, Koji Kamiya, Mayumi Komine, and Mamitaro Ohtsuki. 2021. 'Inflammatory Molecules Associated with Ultraviolet Radiation-Mediated Skin Aging'. *International Journal of Molecular Sciences* 22 (8): 3974. https://doi.org/10.3390/ijms22083974.

Arlt, R. 2008. 'Digitization of Sunspot Drawings by Staudacher in 1749 – 1796'. *Solar Physics* 247 (2): 399–410. https://doi.org/10.1007/s11207-007-9113-4.

Arsenovic, Pavle, Eugene Rozanov, Julien Anet, Andrea Stenke, Werner Schmutz, and Thomas Peter. 2018. 'Implications of Potential Future Grand Solar Minimum for Ozone Layer and Climate'. *Atmospheric Chemistry and Physics* 18 (5): 3469–83. https://doi.org/10.5194/acp-18-3469-2018.

Aucamp, Pieter J., Lars Olof Björn, and Robyn Lucas. 2011. 'Questions and Answers about the Environmental Effects of Ozone Depletion and Its Interactions with Climate Change: 2010 Assessment'. *Photochemical & Photobiological Sciences* 10 (2): 301–16. https://doi.org/10.1039/c0pp90045a.

Austin, John, and R. John Wilson. 2006. 'Ensemble Simulations of the Decline and Recovery of Stratospheric Ozone'. *Journal of Geophysical Research: Atmospheres* 111 (D16): D16314. https://doi.org/10.1029/2005JD006907.

Babatunde, Elisha B., ed. 2012. *Solar Radiation*. InTech Open. https://doi.org/10.5772/1949.

Bais, A. F., G. Bernhard, R. L. McKenzie, P. J. Aucamp, P. J. Young, M. Ilyas, P. Jöckel, and M. Deushi. 2019. 'Ozone—Climate Interactions and Effects on Solar Ultraviolet Radiation'. *Photochemical & Photobiological Sciences* 18 (3): 602–40. https://doi.org/10.1039/c8pp90059k.

Barnard, L., M. Lockwood, M. A. Hapgood, M. J. Owens, C. J. Davis, and F. Steinhilber. 2011. 'Predicting Space Climate Change'. *Geophysical Research Letters* 38 (16): L16103. https://doi.org/10.1029/2011GL048489.

Bazilevskaya, G. A., I. G. Usoskin, E. O. Flückiger, R. G. Harrison, L. Desorgher, R. Bütikofer, M. B. Krainev, et al. 2008. 'Cosmic Ray Induced Ion Production in the Atmosphere'. *Space Science Reviews* 137: 149–73. https://doi.org/10.1007/s11214-008-9339-y.

Benrath, Justus, Frank Gillardon, and Manfred Zimmermann. 2001. 'Differential Time Courses of Skin Blood Flow and Hyperalgesia in the Human Sunburn Reaction Following Ultraviolet Irradiation of the Skin'. *European Journal of Pain* 5 (2): 155–69. https://doi.org/10.1053/eujp.2001.0229.

Bernhard, G., B. Mayer, G. Seckmeyer, and A. Moise. 1997. 'Measurements of Spectral Solar UV Irradiance in tropical-Australia'. *Journal of Geophysical Research: Atmospheres* 102 (D7): 8719–30. https://doi.org/10.1029/97JD00072.

Bhatia, S. C. 2014. 'Solar Radiations'. In *Advanced Renewable Energy Systems*, edited by S. C. Bhatia, 32–67. Woodhead Publishing India. https://doi.org/10.1016/B978-1-78242-269-3.50002-4.

Bikle, Daniel, John Adams, and Sylvia Christakos. 2018. 'Vitamin D: Production, Metabolism, Action, and Clinical Requirements'. In Primer on the Metabolic Bone Diseases and Disorders of Mineral Metabolism, edited by John P. Bilezikian, Roger Bouillon, Thomas Clemens, Juliet Compston, and Douglas C. Bauer, 9th ed., 230–40. Hoboken: Wiley-Blackwell. https://doi.org/10.1002/9781119266594.ch30.

Bornman, Janet F., Paul W. Barnes, T. Matthew Robson, Sharon A. Robinson, Marcel A. K. Jansen, Carlos L. Ballaré, and Stephan D. Flint. 2019. 'Linkages between Stratospheric Ozone, UV Radiation and Climate Change and Their Implications for Terrestrial Ecosystems'. *Photochemical & Photobiological Sciences* 18 (3): 681–716. https://doi.org/10.1039/c8pp90061b.

Bouillon, Roger, John Eisman, M. Garabedian, Michael Holick, J. Kleinschmidt, T. Suda, Irina Terenetskaya, and A. Webb. 2006. 'Action Spectrum for the Production of Previtamin D3 in Human Skin'. *CIE J.* 174 (January):1–12.

Britannica, T. Editors of Encyclopaedia. 2023. 'Sun Worship'. In *Encyclopedia Britannica*. Accessed 29 May 2024. https://www.britannica.com/topic/sun-worship.

Chawda, Dishita, and Pranaykumar Shinde. 2022. 'Effects of Solar Radiation on the Eyes'. *Cureus* 14 (10). e30857. https://doi.org/10.7759/cureus.30857.

Clette, Frédéric, David Berghmans, Petra Vanlommel, Ronald A.M. Van Der Linden, André Koeckelenbergh, and Laurence Wauters. 2007. 'From the Wolf Number to the International Sunspot Index: 25 Years of SIDC'. *Advances in Space Research* 40 (7): 919–28. https://doi.org/10.1016/j.asr.2006.12.045.

De Pinto, Giuseppe, Silvia Mignozzi, Carlo La Vecchia, Fabio Levi, Eva Negri, and Claudia Santucci. 2024. 'Global Trends in Cutaneous Malignant Melanoma Incidence and Mortality'. *Melanoma Research* 34 (3): 265–75. https://doi.org/10.1097/CMR.0000000000000959.

Dessler, Andrew Emory. 2000. *The Chemistry and Physics of Stratospheric Ozone*. International Geophysics Series. San Diego: San Diego Academic Press.

El Ghissassi, Fatiha, Robert Baan, Kurt Straif, Yann Grosse, Béatrice Secretan, Véronique Bouvard, Lamia Benbrahim-Tallaa, et al. 2009. 'A Review of Human Carcinogens--Part D: Radiation'. *The Lancet. Oncology* 10 (8): 751–52. https://doi.org/10.1016/s1470-2045(09)70213-x.

Eldridge, Alison. 2023. '7 Winter Solstice Celebrations From Around the World'. In *Encyclopedia Britannica*. Accessed 29 May 2024. https://www.britannica.com/list/7-winter-solstice-celebrations-from-around-the-world.

Emde, Claudia, Robert Buras-Schnell, Arve Kylling, Bernhard Mayer, Josef Gasteiger, Ulrich Hamann, Jonas Kylling, et al. 2016. 'The libRadtran Software Package for Radiative Transfer Calculations (Version 2.0.1)'. *Geoscientific Model Development* 9 (5): 1647–72. https://doi.org/10.5194/gmd-9-1647-2016.

Farman, J. C., B. G. Gardiner, and J. D. Shanklin. 1985. 'Large Losses of Total Ozone in Antarctica Reveal Seasonal ClOx/NOx Interaction'. *Nature* 315 (6016): 207–10. https://doi.org/10.1038/315207a0.

Feulner, Georg, and Stefan Rahmstorf. 2010. 'On the Effect of a New Grand Minimum of Solar Activity on the Future Climate on Earth'. *Geophysical Research Letters* 37 (5): L05707. https://doi.org/10.1029/2010GL042710.

Flannery, C., L.-A. Burke, L. Grainger, P. Williams, and H. Gage. 2016. 'Risky Sun Tanning Behaviours amongst Irish University Students: A Quantitative Analysis'. *Irish Journal of Medical Science* 185 (4): 887–93. https://doi.org/10.1007/s11845-015-1389-z.

Flo, Ana, Ana C. Calpena, Antoni Díez-Noguera, Alfons Del Pozo, and Trinitat Cambras. 2017. 'Daily Variation of UV-induced Erythema and the Action of Solar Filters'. *Photochemistry and Photobiology* 93 (2): 632–35. https://doi.org/10.1111/php.12670.

Gellén, Emese, Eszter Janka, Ildikó Tamás, Balázs Ádám, Irene Horkay, Gabriella Emri, and Éva Remenyik. 2016. 'Pigmented Naevi and Sun Protection Behaviour among Primary and Secondary School Students in an Eastern Hungarian City'. *Photodermatology, Photoimmunology & Photomedicine* 32 (2): 98–106. https://doi.org/10.1111/phpp.12219.

Gies, Peter, Colin Roy, Simon Toomey, and David Tomlinson. 1999. 'Ambient Solar UVR, Personal Exposure and Protection'. *Journal of Epidemiology* 9 (6): 115–22. https://doi.org/10.2188/jea.9.6sup_115.

Glenn, Beth A., Tiffany Lin, L. Cindy Chang, Ashley Okada, Weng Kee Wong, Karen Glanz, and Roshan Bastani. 2015. 'Sun Protection Practices and Sun Exposure among Children with a Parental History of Melanoma'. *Cancer Epidemiology, Biomarkers & Prevention* 24 (1): 169–77. https://doi.org/10.1158/1055-9965.EPI-14-0650.

Gray, L. J., J. Beer, M. Geller, J. D. Haigh, M. Lockwood, K. Matthes, U. Cubasch, et al. 2010. 'Solar Influences on Climate'. *Reviews of Geophysics* 48 (4): RG4001. https://doi.org/10.1029/2009RG000282.

Gregersen, Erik. 2015. 'Luminosity'. In *Encyclopedia Britannica*. Accessed 29 May 2024. https://www.britannica.com/science/luminosity.

Gupta, Asheesh, Pinar Avci, Tianhong Dai, Ying-Ying Huang, and Michael R. Hamblin. 2013. 'Ultraviolet Radiation in Wound Care: Sterilization and Stimulation'. *Advances in Wound Care* 2 (8): 422–37. https://doi.org/10.1089/wound.2012.0366.

Guy, Gery P., Steven R. Machlin, Donatus U. Ekwueme, and K. Robin Yabroff. 2015. 'Prevalence and Costs of Skin Cancer Treatment in the U.S., 2002-2006 and 2007-2011'. *American Journal of Preventive Medicine* 48 (2): 183–87. https://doi.org/10.1016/j.amepre.2014.08.036.

Hathaway, David H. 2015. 'The Solar Cycle'. *Living Reviews in Solar Physics* 12 (4): 7-87. https://doi.org/10.1007/lrsp-2015-4.

Holick, Michael F. 2001. 'A Perspective on the Beneficial Effects of Moderate Exposure to Sunlight: Bone Health, Cancer Prevention, Mental Health and Well Being'. In *Sun Protection in Man*, edited by Paolo U. Giacomoni, 1st ed. Vol. 3. Comprehensive Series in Photosciences. Amsterdam; New York: Elsevier Science.

Holman, Dawn M., Zahava Berkowitz, Gery P. Guy, Anne M. Hartman, and Frank M. Perna. 2014. 'The Association between Demographic and Behavioral Characteristics and Sunburn among U.S. Adults — National Health Interview Survey, 2010'. *Preventive Medicine* 63 (June): 6–12. https://doi.org/10.1016/j.ypmed.2014.02.018.

Hossain, Eklas. 2023. *The Sun, Energy, and Climate Change*. Cham: Springer Nature Switzerland. https://doi.org/10.1007/978-3-031-22196-5.

Hoyt, Douglas V., and Kenneth H. Schatten. 1998. 'Group Sunspot Numbers: A New Solar Activity Reconstruction'. *Solar Physics* 179 (1): 189–219. https://doi.org/10.1023/A:1005007527816.

Ineson, Sarah, Amanda C. Maycock, Lesley J. Gray, Adam A. Scaife, Nick J. Dunstone, Jerald W. Harder, Jeff R. Knight, Mike Lockwood, James C. Manners, and Richard A. Wood. 2015. 'Regional Climate Impacts of a Possible Future Grand Solar Minimum'. *Nature Communications* 6 (1): 7535. https://doi.org/10.1038/ncomms8535.

International Agency for Research on Cancer, and WHO. n.d. 'Skin Cancer'. International Agency for Research on Cancer. Accessed 9 May 2024. https://www.iarc.who.int/cancer-type/skin-cancer.

IPCC. 2014. *Climate Change 2013: The Physical Science Basis: Working Group I Contribution to the Fifth Assessment Report of the Intergovernmental Panel on Climate Change*. Edited by T. F. Stocker, D. Qin, G.-K. Plattner, M. Tignor, S. K. Allen, J. Boschung, A. Nauels, Y. Xia, V. Bex, and P. M. Midgley. New York: Cambridge University Press.

Jackson, Stephen T., and John P. Rafferty. 2024. 'Little Ice Age'. In *Encyclopedia Britannica*. Accessed 26 April 2024. https://www.britannica.com/science/Little-Ice-Age.

Kovaltsov, Gennady A., and Ilya G. Usoskin. 2010. 'A New 3D Numerical Model of Cosmogenic Nuclide $^{10}$Be Production in the Atmosphere'. *Earth and Planetary Science Letters* 291: 182–88. https://doi.org/10.1016/j.epsl.2010.01.011.

Laschewski, Gudrun, and Andreas Matzarakis. 2023. 'Long-Term Changes of Positive Anomalies of Erythema-Effective UV Irradiance Associated with Low Ozone Events in Germany 1983–2019'. *Environments* 10 (2): 31. https://doi.org/10.3390/environments10020031.

Li, F., R. S. Stolarski, and P. A. Newman. 2009. 'Stratospheric Ozone in the Post-CFC Era'. *Atmospheric Chemistry and Physics* 9 (6): 2207–13. https://doi.org/10.5194/acp-9-2207-2009.

Lockwood, M. 2010. 'Solar Change and Climate: An Update in the Light of the Current Exceptional Solar Minimum'. *Proceedings of the Royal Society A: Mathematical, Physical and Engineering Sciences* 466 (2114): 303–29. https://doi.org/10.1098/rspa.2009.0519.

Lockwood, M., M. J. Owens, L. Barnard, C. J. Davis, and F. Steinhilber. 2011. 'The Persistence of Solar Activity Indicators and the Descent of the Sun into Maunder Minimum Conditions'. *Geophysical Research Letters* 38 (22): L22105. https://doi.org/10.1029/2011GL049811.

Lucas, R. M., T. McMichael, W. Smith, B. K. Armstrong, A. Prüss-Üstün, and World Health Organization. 2006. *Solar Ultraviolet Radiation : Global Burden of Disease from Solar Ultraviolet Radiation*. Environmental Burden of Disease Series 13. Geneva: World Health Organization. https://iris.who.int/handle/10665/43505.

Lucas, R. M., R. E. Neale, S. Madronich, and R McKenzie. 2018. 'Are Current Guidelines for Sun Protection Optimal for Health? Exploring the Evidence'. *Photochemical & Photobiological Sciences* 17 (12): 1956–63. https://doi.org/10.1039/c7pp00374a.

Lucas, R. M., M. Norval, R. E. Neale, A. R. Young, F. R. De Gruijl, Y. Takizawa, and J. C. Van Der Leun. 2014. 'The Consequences for Human Health of Stratospheric Ozone Depletion in Association with Other Environmental Factors'. *Photochemical & Photobiological Sciences* 14 (1): 53–87. https://doi.org/10.1039/c4pp90033b.

Lucas, R. M., A. Prüss-Üstün, and E. Perkins van Deventer. 2010. *Solar Ultraviolet Radiation: Assessing the Environmental Burden of Disease at National and Local Levels*. Edited by World Health Organization. Vol. 17. Environmental Burden of Disease Series. Geneva: World Health Organization. https://iris.who.int/handle/10665/339523.

Lucas, R. M., S. Yazar, A. R. Young, M. Norval, F. R. De Gruijl, Y. Takizawa, L. E. Rhodes, C. A. Sinclair, and R. E. Neale. 2019. 'Human Health in Relation to Exposure to Solar Ultraviolet Radiation under Changing Stratospheric Ozone and Climate'. *Photochemical & Photobiological Sciences* 18 (3): 641–80. https://doi.org/10.1039/c8pp90060d.

Madronich, Sasha, and Siri Flocke. 1999. 'The Role of Solar Radiation in Atmospheric Chemistry'. In *Environmental Photochemistry*, edited by Pierre Boule, 2:1–26. The Handbook of Environmental Chemistry. Berlin, Heidelberg: Springer Berlin Heidelberg. https://doi.org/10.1007/978-3-540-69044-3_1.

Malinović-Milićević, Slavica, Zoran Mijatović, Gorica Stanojević, Milan M. Radovanović, and Vladimir Popović. 2022. 'Health Risks of Extended Exposure to Low-Level UV Radiation – An Analysis of Ground-Based and Satellite-Derived Data'. *Science of The Total Environment* 831 (July):154899. https://doi.org/10.1016/j.scitotenv.2022.154899.

Martin-Puertas, Celia, Katja Matthes, Achim Brauer, Raimund Muscheler, Felicitas Hansen, Christof Petrick, Ala Aldahan, Göran Possnert, and Bas Van Geel. 2012. 'Regional Atmospheric Circulation Shifts Induced by a Grand Solar Minimum'. *Nature Geoscience* 5 (6): 397–401. https://doi.org/10.1038/ngeo1460.

Maycock, A. C., S. Ineson, L. J. Gray, A. A. Scaife, J. A. Anstey, M. Lockwood, N. Butchart, S. C. Hardiman, D. M. Mitchell, and S. M. Osprey. 2015. 'Possible Impacts of a Future Grand Solar Minimum on Climate: Stratospheric and Global Circulation Changes'. *Journal of Geophysical Research: Atmospheres* 120 (18): 9043–58. https://doi.org/10.1002/2014JD022022.

Mayer, B., and A. Kylling. 2005. 'Technical Note: The libRadtran Software Package for Radiative Transfer Calculations - Description and Examples of Use'. *Atmospheric Chemistry and Physics* 5 (7): 1855–77. https://doi.org/10.5194/acp-5-1855-2005.

Meehl, Gerald A., Julie M. Arblaster, and Daniel R. Marsh. 2013. 'Could a Future "Grand Solar Minimum" like the Maunder Minimum Stop Global Warming?' *Geophysical Research Letters* 40 (9): 1789–93. https://doi.org/10.1002/grl.50361.

Moysan, Annie, Isabelle Marquis, François Gaboriau, René Santus, Louis Dubertret, and Patrice Morlière. 1993. 'Ultraviolet A – Induced Lipid Peroxidation and Antioxidant Defense Systems in Cultured Human Skin Fibroblasts'. *Journal of Investigative Dermatology* 100 (5): 692–98. https://doi.org/10.1111/1523-1747.ep12472352.

Muthers, S., J. G. Anet, A. Stenke, C. C. Raible, E. Rozanov, S. Brönnimann, T. Peter, et al. 2014. 'The Coupled Atmosphere–Chemistry–Ocean Model SOCOL-MPIOM'. *Geoscientific Model Development* 7 (5): 2157–79. https://doi.org/10.5194/gmd-7-2157-2014.

Nahar, Vinayak K., M. Allison Ford, Robert T. Brodell, Javier F. Boyas, Stephanie K. Jacks, Rizwana Biviji-Sharma, Mary A. Haskins, and Martha A. Bass. 2016. 'Skin Cancer Prevention Practices among Malignant Melanoma Survivors: A Systematic Review'. *Journal of Cancer Research and Clinical Oncology* 142 (6): 1273–83. https://doi.org/10.1007/s00432-015-2086-z.

NASA Science Editorial Team. 2013. 'Solar Variability and Terrestrial Climate'. NASA Science. 7 January 2013. Accessed 25 April 2024. https://science.nasa.gov/science-research/planetary-science/08jan_sunclimate/.

———. 2017. 'Solar Minimum Is Coming'. NASA Science. 27 June 2017. Accessed 29 April 2024. https://science.nasa.gov/science-research/planetary-science/solar-minimum-is-coming/.

———. 2019. ‘What Is the Sun’s Role in Climate Change?’ NASA Science. 6 September 2019. Accessed 29 April 2024. https://science.nasa.gov/earth/climate-change/what-is-the-suns-role-in-climate-change/.

———. 2020. ‘There Is No Impending “Mini Ice Age”’. NASA Science. 13 February 2020. Accessed 26 April 2024. https://science.nasa.gov/earth/climate-change/there-is-no-impending-mini-ice-age/.

National Institutes of Health Office of Dietary Supplements. 2023. ‘Vitamin D: Fact Sheet for Health Professionals’. NIH: Office of Dietary Supplements. 18 September 2023. Accessed 9 May 2024. https://ods.od.nih.gov/factsheets/VitaminD-HealthProfessional/.

National research council, ed. 2012. *The Effects of Solar Variability on Earth’s Climate: A Workshop Report*. Washington: National academies press.

Neale, R.E., S.R. Khan, R.M. Lucas, M. Waterhouse, D.C. Whiteman, and C.M. Olsen. 2019. ‘The Effect of Sunscreen on Vitamin D: A Review’. *British Journal of Dermatology* 181 (5): 907–15. https://doi.org/10.1111/bjd.17980.

Olsen, Catherine M., Louise F. Wilson, Adele C. Green, Christopher J. Bain, Lin Fritschi, Rachel E. Neale, and David C. Whiteman. 2015. ‘Cancers in Australia Attributable to Exposure to Solar Ultraviolet Radiation and Prevented by Regular Sunscreen Use’. *Australian and New Zealand Journal of Public Health* 39 (5): 471–76. https://doi.org/10.1111/1753-6405.12470.

Ostberg, René. 2023. ‘Midsummer’. In *Encyclopedia Britannica*. Accessed 29 May 2024. https://www.britannica.com/topic/Midsummer-holiday.

Rapp, Donald. 2010. *Assessing Climate Change: Temperatures, Solar Radiation, and Heat Balance*. 2. ed. [updated and rev.]. Springer-Praxis Books in Environmental Sciences. Berlin Heidelberg: Springer.

Rastogi, Rajesh P., Richa, Ashok Kumar, Madhu B. Tyagi, and Rajeshwar P. Sinha. 2010. ‘Molecular Mechanisms of Ultraviolet Radiation-Induced DNA Damage and Repair’. *Journal of Nucleic Acids* 2010:1–32. https://doi.org/10.4061/2010/592980.

Raymond-Lezman, Jonathan R, and Suzanne Riskin. 2023. ‘Attitudes, Behaviors, and Risks of Sun Protection to Prevent Skin Cancer Amongst Children, Adolescents, and Adults’. *Cureus* 15 (2): e34934. https://doi.org/10.7759/cureus.34934.

Roth, R., and F. Joos. 2013. ‘A Reconstruction of Radiocarbon Production and Total Solar Irradiance from the Holocene $^{14}C$ and $CO_2$; Records: Implications of Data and Model Uncertainties’. *Climate of the Past* 9 (4): 1879–1909. https://doi.org/10.5194/cp-9-1879-2013.

Rozanov, Eugene V., Tatiana A. Egorova, Alexander I. Shapiro, and Werner K. Schmutz. 2011. ‘Modeling of the Atmospheric Response to a Strong Decrease of the Solar Activity’. *Proceedings of the International Astronomical Union* 7 (S286): 215–24. https://doi.org/10.1017/S1743921312004863.

Samaniego-Rascón, Danyela, Manuel C. Gameiro da Silva, Almerindo D. Ferreira, and Rafael E. Cabanillas-Lopez. 2019. ‘Solar Energy Industry Workers under Climate Change: A Risk Assessment of the Level of Heat Stress Experienced by a Worker Based on Measured Data’. *Safety Science* 118 (October):33–47. https://doi.org/10.1016/j.ssci.2019.04.042.

Satagopan, Jaya M., Susan A. Oliveria, Arshi Arora, Michael A. Marchetti, Irene Orlow, Stephen W. Dusza, Martin A. Weinstock, et al. 2015. 'Sunburn, Sun Exposure, and Sun Sensitivity in the Study of Nevi in Children'. *Annals of Epidemiology* 25 (11): 839-843. https://doi.org/10.1016/j.annepidem.2015.05.004.

Schuch, André Passaglia, Camila Carriao Machado Garcia, Kazuo Makita, and Carlos Frederico Martins Menck. 2013. 'DNA Damage as a Biological Sensor for Environmental Sunlight'. *Photochemical & Photobiological Sciences* 12 (8): 1259–72. https://doi.org/10.1039/c3pp00004d.

Schuessler, Manfred. 2007. 'Are Solar Cycles Predictable?' *Astronomische Nachrichten* 328 (10): 1087–91. https://doi.org/10.1002/asna.200710836.

Setlow, R. B. 1974. 'The Wavelengths in Sunlight Effective in Producing Skin Cancer: A Theoretical Analysis'. *Proceedings of the National Academy of Sciences* 71 (9): 3363–66. https://doi.org/10.1073/pnas.71.9.3363.

Shapiro, A. I., W. Schmutz, E. Rozanov, M. Schoell, M. Haberreiter, A. V. Shapiro, and S. Nyeki. 2011. 'A New Approach to the Long-Term Reconstruction of the Solar Irradiance Leads to Large Historical Solar Forcing'. *Astronomy & Astrophysics* 529 (May): A67. https://doi.org/10.1051/0004-6361/201016173.

Shepherd, Theodore G. 2008. 'Dynamics, Stratospheric Ozone, and Climate Change'. *Atmosphere-Ocean* 46 (1): 117–38. https://doi.org/10.3137/ao.460106.

Sinha, Rajeshwar P., and Donat P. Häder. 2002. 'UV-Induced DNA Damage and Repair: A Review'. *Photochemical & Photobiological Sciences: Official Journal of the European Photochemistry Association and the European Society for Photobiology* 1 (4): 225–36. https://doi.org/10.1039/b201230h.

Sklar, Lindsay R., Fahad Almutawa, Henry W. Lim, and Iltefat Hamzavi. 2012. 'Effects of Ultraviolet Radiation, Visible Light, and Infrared Radiation on Erythema and Pigmentation: A Review'. *Photochemical & Photobiological Sciences* 12 (1): 54–64. https://doi.org/10.1039/c2pp25152c.

Solomon, Susan. 2019. 'The Discovery of the Antarctic Ozone Hole'. *Nature* 575 (7781): 46–47. https://doi.org/10.1038/d41586-019-02837-5.

Stamnes, Knut, Gary E. Thomas, and Jakob J. Stamnes. 2017. *Radiative Transfer in the Atmosphere and Ocean*. 2nd ed. Cambridge: Cambridge University Press. https://doi.org/10.1017/9781316148549.

Steinhilber, Friedhelm, Jose A. Abreu, Jürg Beer, Irene Brunner, Marcus Christl, Hubertus Fischer, Ulla Heikkilä, et al. 2012. '9,400 Years of Cosmic Radiation and Solar Activity from Ice Cores and Tree Rings'. *Proceedings of the National Academy of Sciences* 109 (16): 5967–71. https://doi.org/10.1073/pnas.1118965109.

Steinhilber, Friedhelm, and Jürg Beer. 2013. 'Prediction of Solar Activity for the next 500 Years'. *Journal of Geophysical Research: Space Physics* 118 (5): 1861–67. https://doi.org/10.1002/jgra.50210.

Sulzberger, B., A. T. Austin, R. M. Cory, R. G. Zepp, and N. D. Paul. 2019. 'Solar UV Radiation in a Changing World: Roles of Cryosphere—Land—Water—Atmosphere Interfaces in Global Biogeochemical Cycles'. *Photochemical & Photobiological Sciences* 18 (3): 747–74. https://doi.org/10.1039/c8pp90063a.

Symanzik, Cara, and Swen Malte John. 2022. 'Sun Protection and Occupation: Current Developments and Perspectives for Prevention of Occupational Skin Cancer'. *Frontiers in Public Health* 10 (December):1110158. https://doi.org/10.3389/fpubh.2022.1110158.

Taylor, Myra F., Dominique Westbrook, and Paul Chang. 2016. 'Using UV Photoaged Photography to Better Understand Western Australian Teenagers' Attitudes towards Adopting Sun-Protective Behaviors'. *International Journal of Adolescent Medicine and Health* 28 (1): 45–53. https://doi.org/10.1515/ijamh-2014-0071.

TEMIS, and Royal Netherlands Meteorological Institute. 2022. 'UV Index and UV Dose: Short Introduction'. Tropospheric Emission Monitoring Internet Service. 21 February 2022. Accessed 22 May 2024. https://www.temis.nl/uvradiation/info/index.html.

Tetreau, Guillaume, Alexia Chandor-Proust, Frédéric Faucon, Renaud Stalinski, Idir Akhouayri, Sophie M. Prud'homme, Myriam Régent-Kloeckner, Muriel Raveton, and Stéphane Reynaud. 2014. 'UV Light and Urban Pollution: Bad Cocktail for Mosquitoes?' *Aquatic Toxicology* 146 (January): 52–60. https://doi.org/10.1016/j.aquatox.2013.10.031.

Thomas, Vanessa. 2020. 'What Will Solar Cycle 25 Look Like?' NASA Science. 17 September 2020. Accessed 29 April 2024. https://www.nasa.gov/missions/sdo/what-will-solar-cycle-25-look-like/.

Urbach, Frederick. 2001. 'The Negative Effects of Solar Radiation: A Clinical Overview'. In *Sun Protection in Man*, edited by Paolo U. Giacomoni, 1st ed, 3:39–67. Comprehensive Series in Photosciences. Amsterdam; New York: Elsevier Science.

Usoskin, I. G. 2023. 'A History of Solar Activity over Millennia'. *Living Reviews in Solar Physics* 20 (2): 1-113. https://doi.org/10.1007/s41116-023-00036-z.

Usoskin, I. G., S. K. Solanki, and M. Korte. 2006. 'Solar Activity Reconstructed over the Last 7000 Years: The Influence of Geomagnetic Field Changes'. *Geophysical Research Letters* 33 (8): L08103. https://doi.org/10.1029/2006GL025921.

Usoskin, I. G., S. K. Solanki, and G. Kovaltsov. 2011. 'Grand Minima of Solar Activity during the Last Millennia'. *Proceedings of the International Astronomical Union* 7 (S286): 372–82. https://doi.org/10.1017/S174392131200511X.

Usoskin, I. G., S. K. Solanki, and G. A. Kovaltsov. 2007. 'Grand Minima and Maxima of Solar Activity: New Observational Constraints'. *Astronomy & Astrophysics* 471 (1): 301–9. https://doi.org/10.1051/0004-6361:20077704.

Väisänen, Pauli, Ilya Usoskin, Riikka Kähkönen, Sergey Koldobskiy, and Kalevi Mursula. 2023. 'Revised Reconstruction of the Heliospheric Modulation Potential for 1964–2022'. *Journal of Geophysical Research: Space Physics* 128 (4): e2023JA031352. https://doi.org/10.1029/2023JA031352.

Van Dijk, Arjan, Harry Slaper, Peter N. Den Outer, Olaf Morgenstern, Peter Braesicke, John A. Pyle, Hella Garny, et al. 2013. 'Skin Cancer Risks Avoided by the Montreal Protocol—Worldwide Modeling Integrating Coupled Climate-

Chemistry Models with a Risk Model for UV'. *Photochemistry and Photobiology* 89 (1): 234–46. https://doi.org/10.1111/j.1751-1097.2012.01223.x.

Van Geffen, Jos, Michiel Van Weele, Marc Allaart, and Ronald Van Der A. 2017. 'TEMIS UV Index and UV Dose MSR-2 Data Products, Version 2'. Dataset. Royal Netherlands Meteorological Institute (KNMI). https://doi.org/10.21944/TEMIS-UV-MSR2-V2.

Vaquero, J. M. 2007. 'Historical Sunspot Observations: A Review'. *Advances in Space Research* 40 (7): 929–41. https://doi.org/10.1016/j.asr.2007.01.087.

Waugh, Darryn. 2009. 'The Age of Stratospheric Air'. *Nature Geoscience* 2 (1): 14–16. https://doi.org/10.1038/ngeo397.

Webb, Ann R., Harry Slaper, Peter Koepke, and Alois W. Schmalwieser. 2011. 'Know Your Standard: Clarifying the CIE Erythema Action Spectrum'. *Photochemistry and Photobiology* 87 (2): 483–86. https://doi.org/10.1111/j.1751-1097.2010.00871.x.

WHO. 2022. 'Ultraviolet Radiation'. World Health Organization. 21 June 2022. Accessed 21 May 2024. https://www.who.int/news-room/fact-sheets/detail/ultraviolet-radiation.

Williamson, Craig E., Patrick J. Neale, Samuel Hylander, Kevin C. Rose, Félix L. Figueroa, Sharon A. Robinson, Donat-P. Häder, Sten-Åke Wä, and Robert C. Worrest. 2019. 'The Interactive Effects of Stratospheric Ozone Depletion, UV Radiation, and Climate Change on Aquatic Ecosystems'. *Photochemical & Photobiological Sciences* 18 (3): 717–46. https://doi.org/10.1039/c8pp90062k.

Wilson, S. R., S. Madronich, J. D. Longstreth, and K. R. Solomon. 2019. 'Interactive Effects of Changing Stratospheric Ozone and Climate on Tropospheric Composition and Air Quality, and the Consequences for Human and Ecosystem Health'. *Photochemical & Photobiological Sciences* 18 (3): 775–803. https://doi.org/10.1039/c8pp90064g.

World Meteorological Organization. 2022. 'Executive Summary. Scientific Assessment of Ozone Depletion: 2022'. 278. GAW Report. Geneva: World Meteorological Organization (WMO). https://library.wmo.int/idurl/4/42105.

Yang, Jing-Wen, Guo-Biao Fan, Fei Tan, Hai-Mei Kong, Qing Liu, Ying Zou, and Yi-Mei Tan. 2023. 'The Role and Safety of UVA and UVB in UV-Induced Skin Erythema'. *Frontiers in Medicine* 10 (June):1163697. https://doi.org/10.3389/fmed.2023.1163697.

Zharkova, Valentina. 2020. 'Modern Grand Solar Minimum Will Lead to Terrestrial Cooling'. *Temperature* 7 (3): 217–22. https://doi.org/10.1080/23328940.2020.1796243.

Zubov, V., E. Rozanov, T. Egorova, I. Karol, and W. Schmutz. 2013. 'Role of External Factors in the Evolution of the Ozone Layer and Stratospheric Circulation in 21st Century'. *Atmospheric Chemistry and Physics* 13 (9): 4697–4706. https://doi.org/10.5194/acp-13-4697-2013.

# List of Tables

# List of Figures